Nitrate-Dependent Control of Shoot K Homeostasis by the Nitrate Transporter1/Peptide Transporter Family Member NPF7.3/NRT1.5 and the Stelar K^+ Outward Rectifier SKOR in Arabidopsis[1][OPEN]

Navina Drechsler[2], Yue Zheng[2], Anne Bohner, Barbara Nobmann[3], Nicolaus von Wirén, Reinhard Kunze*, and Christine Rausch

Institute of Biology/Applied Genetics, Dahlem Centre of Plant Sciences, Freie Universität Berlin, D–14195 Berlin, Germany (N.D., Y.Z., B.N., R.K., C.R.); and Molecular Plant Nutrition, Department of Physiology and Cell Biology, Leibniz Institute for Plant Genetics and Crop Plant Research, 06466 Gatersleben, Germany (A.B., N.v.W.)

ORCID IDs: 0000-0002-2431-101X (A.B.); 0000-0002-4966-425X (N.v.W.); 0000-0002-3304-5550 (R.K.).

Root-to-shoot translocation and shoot homeostasis of potassium (K) determine nutrient balance, growth, and stress tolerance of vascular plants. To maintain the cation-anion balance, xylem loading of K^+ in the roots relies on the concomitant loading of counteranions, like nitrate (NO_3^-). However, the coregulation of these loading steps is unclear. Here, we show that the bidirectional, low-affinity Nitrate Transporter1 (NRT1)/Peptide Transporter (PTR) family member NPF7.3/NRT1.5 is important for the NO_3^--dependent K^+ translocation in Arabidopsis (*Arabidopsis thaliana*). Lack of NPF7.3/NRT1.5 resulted in K deficiency in shoots under low NO_3^- nutrition, whereas the root elemental composition was unchanged. Gene expression data corroborated K deficiency in the *nrt1.5-5* shoot, whereas the root responded with a differential expression of genes involved in cation-anion balance. A grafting experiment confirmed that the presence of NPF7.3/NRT1.5 in the root is a prerequisite for proper root-to-shoot translocation of K^+ under low NO_3^- supply. Because the depolarization-activated Stelar K^+ Outward Rectifier (SKOR) has previously been described as a major contributor for root-to-shoot translocation of K^+ in Arabidopsis, we addressed the hypothesis that NPF7.3/NRT1.5-mediated NO_3^- translocation might affect xylem loading and root-to-shoot K^+ translocation through SKOR. Indeed, growth of *nrt1.5-5* and *skor-2* single and double mutants under different K/NO_3^- regimes revealed that both proteins contribute to K^+ translocation from root to shoot. SKOR activity dominates under high NO_3^- and low K^+ supply, whereas NPF7.3/NRT1.5 is required under low NO_3^- availability. This study unravels nutritional conditions as a critical factor for the joint activity of SKOR and NPF7.3/NRT1.5 for shoot K homeostasis.

[1] This work was supported by the Studienstiftung des Deutschen Volkes (N.D.), the China Scholarship Council (Y.Z.), and the Deutsche Forschungsgemeinschaft (Forschergruppe FOR 948 grant nos. WI1728/14–2 to N.v.W. and KU715/10–2 to R.K. and C.R.).

[2] These authors contributed equally to the article.

[3] Present address: Max Planck Institute of Molecular Plant Physiology, Gene Regulatory Networks Group, Wissenschaftspark Golm, Am Mühlenberg 1, 14476 Potsdam, Germany.

* Address correspondence to reinhard.kunze@fu-berlin.de.

The author responsible for distribution of materials integral to the findings presented in this article in accordance with the policy described in the Instructions for Authors (www.plantphysiol.org) is: Reinhard Kunze (reinhard.kunze@fu-berlin.de).

N.D. performed the research (phenotypic, physiological, and expression analyses and grafting experiments), analyzed the data, and wrote the article; Y.Z. performed the research (phenotypic and physiological analyses and yeast experiments), analyzed the data, and wrote the article; A.B. performed the research (hydroponics) and analyzed the data; B.N. performed the research (phenotypic analysis); N.v.W. supervised part of the research and wrote the article; R.K. designed the research, analyzed and interpreted the data, and wrote the article; C.R. designed the research, performed the research (phenotypic and physiological analyses), supervised the research, analyzed and interpreted the data, and wrote the article.

[OPEN] Articles can be viewed without a subscription.
www.plantphysiol.org/cgi/doi/10.1104/pp.15.01152

The macronutrient potassium (K) is essential for plant growth and development because of its crucial roles in various cellular processes (i.e. regulation of enzyme activities), stabilization of protein synthesis, and neutralization of negative charges. In addition, it is a major component of the cation-anion balance and osmoregulation in plants, thereby influencing cellular turgor, xylem and phloem transport, pH homeostasis, and the setting of membrane potentials (Maathuis, 2009; Marschner, 2012; Sharma et al., 2013). K^+ uptake and distribution in Arabidopsis (*Arabidopsis thaliana*) are accomplished by a total of 71 membrane proteins that have been assigned to five gene families: the Shaker and Tandem-Pore K^+ channels (now also including the inward-rectifier K-like (K_{ir}-like) channels), the K^+ uptake permeases (KUP/HAK/KT), the K^+ transporter (HKT) family, and the cation proton antiporters (CPA; Gierth and Mäser, 2007; Gomez-Porras et al., 2012; Sharma et al., 2013).

Root xylem loading is a key step for the delivery of nutrients to the shoot (Poirier et al., 1991; Engels and Marschner, 1992a; Gaymard et al., 1998; Takano et al., 2002; Park et al., 2008). Root-to-shoot translocation of K^+ is mediated by the voltage-dependent Shaker family K^+ channel Stelar K^+ Outward Rectifier (SKOR). The gene is primarily expressed in pericycle and root xylem

parenchyma cells, and it is down-regulated upon K shortage and in response to treatments with the phytohormones abscisic acid, cytokinin, and auxin. Such gene expression changes are thought to control K^+ secretion into the xylem sap and K^+ reallocation through the phloem to adjust root K^+ transport activity to K^+ availability and shoot demand (Pilot et al., 2003). SKOR is activated upon membrane depolarization, and it is in a closed state when the driving force for K^+ is inwardly directed. It elicits outward K^+ currents, facilitating the release of the cation from the cells into the xylem. The voltage dependency of the channel is modulated by the external K^+ concentration to minimize the risk of an undesired K^+ influx under high K^+ availability (Johansson et al., 2006). Root-to-shoot K^+ transfer was strongly reduced in the knockout mutant *skor-1*, resulting in a decreased shoot K content, whereas the root K content remained unaffected (Gaymard et al., 1998).

Root xylem loading is subject to the maintenance of a cation-anion balance, and nitrate (NO_3^-) is the quantitatively most important anion counterbalancing xylem loading of K^+ (Engels and Marschner, 1993). Members of the Nitrate Transporter1 (NRT1)/Peptide Transporter (PTR) transporter family (NPF) play a prominent role in NO_3^- uptake and allocation in Arabidopsis (summarized in Krouk et al., 2010; Wang et al., 2012; and Léran et al., 2014). Two of them have recently been reported to control xylem NO_3^- loading and unloading. The low-affinity, pH-dependent bidirectional NO_3^- transporter NPF7.3/NRT1.5 (subsequently termed NRT1.5) mediates NO_3^- efflux from pericycle cells to the xylem vessels, whereas the low-affinity influx protein NPF7.2/NRT1.8 removes NO_3^- from the xylem sap and transfers it into xylem parenchyma cells (Lin et al., 2008; Li et al., 2010; Chen et al., 2012). Accordingly, the expression of both genes is oppositely regulated under various stress conditions (Li et al., 2010). In *nrt1.5* mutants, *NRT1.8* expression is increased, which is thought to enhance NO_3^- reallocation to the root (Chen et al., 2012).

The *NRT1.5* gene is mainly expressed in root pericycle cells close to the xylem, and the protein localizes to the plasma membrane. In *nrt1.5* mutants, less NO_3^- is transported from the root to the shoot, and the NO_3^- concentration in the xylem sap is reduced. However, root-to-shoot NO_3^- transport is not completely abolished in these mutants, indicating the existence of additional xylem-loading activities for NO_3^- (Lin et al., 2008; Wang et al., 2012). The recent observation that NPF6.3/NRT1.1/CHL1 and NPF6.2/NRT1.4 are also capable of mediating bidirectional NO_3^- transport in *Xenopus laevis* oocytes might indicate that more NPF family members are contributing to xylem loading with NO_3^- (Léran et al., 2013).

Electrophysiological studies with *NRT1.5*-expressing *X. laevis* oocytes revealed that NO_3^- excited an inward current at pH 5.5, which would be expected for a proton-coupled nitrate transporter with a proton to nitrate ratio larger than one (Lin et al., 2008). The inward currents elicited by exposure to nitrate were pH dependent, and Lin et al. (2008) observed that NRT1.5 can also facilitate nitrate efflux when the oocytes were incubated at pH 7.4. Lin et al. (2008) concluded that NRT1.5 can transport nitrate in both directions, presumably through a proton-coupled mechanism. Interestingly, a K^+ gradient was not sufficient to drive NRT1.5-mediated NO_3^- export. However, the determination of root and shoot cation concentrations in the *nrt1.5-1* mutant revealed that the amount of K^+ translocated to the shoot was reduced when NO_3^- but not NH_4^+ was supplied as the N source. Therefore, Lin et al. (2008) suggested a regulatory loop between NO_3^- and K^+ at the xylem loading step.

A close relationship between these two nutrients concerning uptake, translocation, recycling, and reduction (of NO_3^-) has been described in physiological studies since the 1960s (e.g. Ben Zioni et al., 1971; Blevins et al., 1978; Barneix and Breteler, 1985), but only recently, common components in the NO_3^- and K^+ uptake pathways were identified and led to the first ideas of how such a cross talk might be coordinated on the molecular level. The uptake activity of the K^+ channel AKT1 as well as the affinity of the NO_3^- transporter NPF6.3/NRT1.1/CHL1 are both modulated by the activity of CALCINEURIN B-LIKE PROTEIN-INTERACTING PROTEIN KINASE23 (CIPK23), which itself is regulated by CALCINEURIN B-LIKE PROTEIN9 (CBL9) under both deficiencies (Xu et al., 2006; Ho et al., 2009). Yet, the details of this interaction in root K^+ uptake, the (regulation of) xylem loading with K^+ and NO_3^-, and the involvement of SKOR and NRT1.5 in this process are unknown.

In this study, we approached this problem by investigating the molecular and physiological responses of Arabidopsis wild-type (Columbia-0 [Col-0]), *nrt1.5*, and *skor* transfer DNA (T-DNA) insertion lines to varying NO_3^- and K^+ regimes. The *nrt1.5* mutant developed an early senescence phenotype under low NO_3^- nutrition, which could be attributed to a reduced K^+ translocation to the shoot. The assessment of *nrt1.5* and *skor* single- and double-knockout lines disclosed an interplay of the two proteins in the NO_3^--dependent control of shoot K homeostasis. The presented data indicate that SKOR mediates K^+ root-to-shoot translocation under high NO_3^- and low K^+ availability, whereas NRT1.5 is important for K^+ translocation under low NO_3^- availability, irrespective of the K^+ supply.

RESULTS

nrt1.5-5 Mutant Plants Exhibit a Pleiotropic Phenotype on Low-Fertilized Soil

Arabidopsis *nrt1.5* mutant plants are phenotypically indistinguishable from wild-type plants under standard growth conditions (Lin et al., 2008; Chen et al., 2012). However, we found that, on low-fertilized soil, the three mutant lines *nrt1.5-5*, carrying a T-DNA insertion in exon 5 and lacking full-length *NRT1.5* transcripts (Fig. 1, A and B), *nrt1.5-2* (Lin et al., 2008), and *nrt1.5-4* (Li et al., 2010) exhibited the same phenotype (Supplemental Fig. S1). We, therefore, focused subsequent analyses on line *nrt1.5-5*. Until bolting, the plants

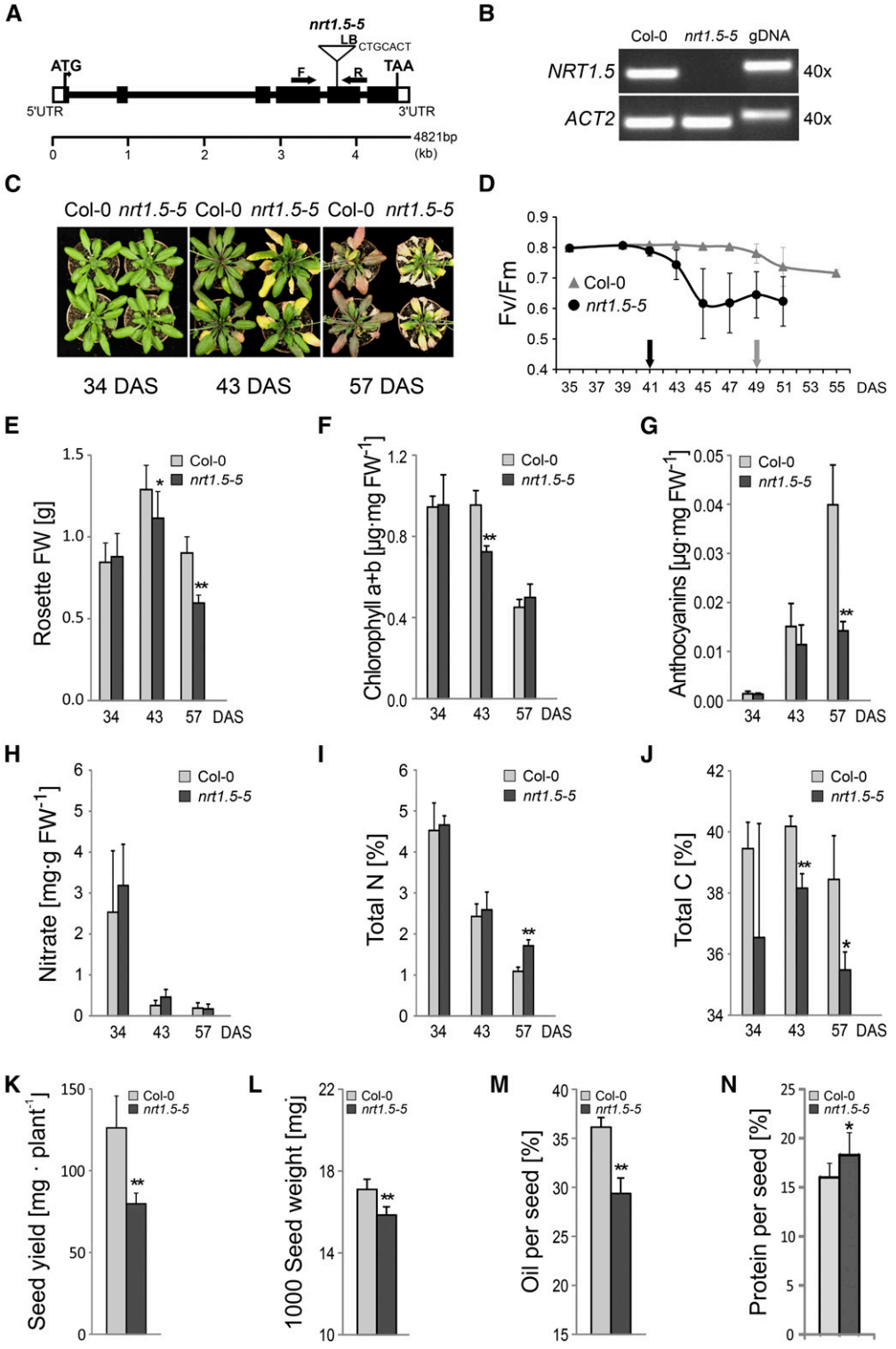

Figure 1. Pleiotropic phenotype of the T-DNA insertion mutant *nrt1.5-5* on low-fertilized soil. A, *NRT1.5* gene structure and T-DNA insertion site of the mutant line *nrt1.5-5*. LB, Left border. White boxes indicate untranslated regions (UTRs), and black boxes indicate exons. Arrows indicate positions of PCR primers used in B. B, RT-PCR analysis of *NRT1.5* transcripts in rosette leaves of wild-type (Col-0) and homozygous *nrt1.5-5* mutant plants. RT-PCR of *ACTIN2* (*ACT2*; At3g18780) and PCR on genomic DNA (gDNA) served as controls. PCR cycle count was 40. C, Early leaf senescence phenotype of *nrt1.5-5* on low-fertilized soil. Growth responses of Col-0 and *nrt1.5-5* plants at 34, 43, and 57 DAS are shown. In three repeats of the experiment, plants developed the same phenotype. D, PSII maximum quantum efficiency

grew without any visible symptoms (Fig. 1C, 34 d after sowing [DAS]). In the following days, tips of old *nrt1.5-5* leaves turned yellow and died, whereas the corresponding leaves of Col-0 plants developed a brown-reddish color and remained turgescent until 57 DAS (Fig. 1C, 43 and 57 DAS). The maximum quantum efficiency of PSII (maximum photochemical efficiency of PSII in the dark-adapted state [F_v/F_m]) was determined as an indicator for senescence initiation and progression in leaf number 8 (Fig. 1D). F_v/F_m declined earlier and faster in *nrt1.5-5* than in Col-0. At 53 DAS, all leaves number 8 in the mutant were dead, whereas the wild-type leaves were still photosynthetically active. Determination of the rosette fresh weight revealed an earlier fresh weight loss of *nrt1.5-5* plants, which coincided with the early senescence symptoms of the leaves (Fig. 1E). Leaf yellowing was reflected by decreased chlorophyll concentrations in the *nrt1.5-5* whole rosettes at 43 DAS (Fig. 1F). At 57 DAS, mutant and wild-type plants contained similar amounts of the pigment. At this time point, the old *nrt1.5-5* leaves were completely dried out, and only the inner part of the mutant rosette appeared light green and turgescent (Fig. 1C). The brown-reddish color of Col-0 rosettes at 57 DAS was the result of an increased anthocyanin production, which did not occur to such an extent in the mutant (Fig. 1G).

Accelerated chlorophyll degradation is usually accompanied by N remobilization from chloroplasts (Hörtensteiner and Feller, 2002) and might be caused by N deficiency in *nrt1.5-5*. To address this issue, we determined NO_3^- and total N concentrations in the rosette material. The measurements revealed that the plants depleted their endogenous NO_3^- reserves in the leaves between 34 and 43 DAS to compensate for the reduced root supply on low-fertilized soil, but a significant difference in the NO_3^- concentrations was not observed between *nrt1.5-5* and Col-0 (Fig. 1H). In contrast, mutant plants contained slightly more total N in their rosettes than the wild type at 57 DAS (Fig. 1I). In addition, the total C content was significantly decreased in *nrt1.5-5* at 43 and 57 DAS (Fig. 1J). This observation was consistent with the early F_v/F_m decline and the lower photosynthetic activity of the mutant (Fig. 1D). The seed yield of *nrt1.5-5* plants was reduced to only 63% relative to the wild type (Fig. 1K), and a significant seed weight reduction was observed (Fig. 1L). The reduced availability of carbon skeletons in *nrt1.5-5* (Fig. 1J) might be the reason for the significantly lower seed oil content (Fig. 1M), whereas the total protein content in dry seeds was even slightly increased (Fig. 1N).

Supplementation of the low-fertilized soil with 10 mM KNO_3 from 34 to 57 DAS diminished or even abolished symptom development of the *nrt1.5-5* mutant (Supplemental Fig. S2). In both wild-type and mutant plants, additional KNO_3 provision resulted in higher biomass production, later chlorophyll degradation, reduced anthocyanin accumulation, increased NO_3^- and total N concentrations at 43 and 57 DAS, and doubling of the seed yield. These results indicated that the pleiotropic phenotype of *nrt1.5-5* was caused by the low KNO_3 fertilization of the soil. NO_3^- and total N concentrations in *nrt1.5-5* were close to wild-type levels under both cultivation conditions (Fig. 1, H and I; Supplemental Fig. S2, F and G), suggesting that K deficiency might be causal for the differential progression of leaf senescence in the mutant. Because Lin et al. (2008) did not report a similar phenotype for the *nrt1.5* mutant plants when grown in hydroponic solutions containing high NO_3^- concentrations (4–12.5 mM), we hypothesized that the putative K deficiency symptoms in old leaves might depend on a limited NO_3^- supply.

Limited NO_3^- Supply to *nrt1.5-5* Plants Causes K Deficiency in Shoot Organs

By subjecting *nrt1.5-5* mutant and Col-0 plants to limiting NO_3^- nutrition (0.1 mM) in hydroponic culture, we addressed the question if low NO_3^- fertilization causes K deficiency in the mutant shoot. As a result of the treatment, *nrt1.5-5* leaves became earlier senescent than the wild type (Fig. 2, A and B), with the outcome of a significant fresh weight reduction in old leaves (Fig. 2C, leaves 1–12). Like in soil-grown mutants (Fig. 1J), total C was slightly (but not significantly) reduced in rosette leaves (Fig. 2D), and total N was elevated in young leaves (nos. ≥13) and roots (Fig. 2E). In comparison with Col-0 plants, all *nrt1.5-5* organs, except the inflorescence stems, contained more NO_3^-, although the concentrations were generally close to the detection limit as a result of the limited NO_3^- supply (Fig. 2F).

When we determined the concentrations of mineral elements by inductively coupled plasma optical emission spectrometry (ICP-OES), most of the macroelements were increased in *nrt1.5-5* leaves with the exception of K (Table I). K concentrations remained below 30% and 50% of the wild-type levels in leaves numbers 1 to 12 and ≥13, corresponding to <1% and <2% of the dry weight, respectively. Because the critical K concentration for plant growth is in the range of 0.5% to 2% (Leigh and Jones, 1984), *nrt1.5-5* rosette leaves experienced K deficiency,

Figure 1. (*Continued.*)
decline in leaf number 8. Black and gray arrows indicate first declines in F_v/F_m in *nrt1.5-5* and Col-0 plants, respectively, indicating senescence initiation (means ± SD; $n = 8$). E, Rosette fresh weight (FW) of Col-0 and *nrt1.5-5* at 34, 43, and 57 DAS (means ± SD; $n = 8$). F, Chlorophyll content decreases at 43 DAS in *nrt1.5-5* whole rosettes but not in Col-0 (means ± SD; $n = 3$). G, Reduced anthocyanin accumulation in *nrt1.5-5* leaves (means ± SD; $n = 3$). H, Nitrate content in rosettes (means ± SD; $n \geq 5$), I, Total N content in rosettes (means ± SD; $n \geq 4$). J, Total C content in rosettes (means ± SD; $n \geq 4$). K, Quantification of seed yield (means ± SD; $n = 8$). L, Thousand-seed weight (means ± SD; $n = 8$). M, Seed oil content (means ± SD; $n = 8$). N, Seed protein content (means ± SD; $n = 8$). Similar results were obtained in two independent experiments. *, Significant differences (Student's *t* test) between *nrt1.5-5* and Col-0 with $P < 0.05$; **, significant differences (Student's *t* test) between *nrt1.5-5* and Col-0 with $P < 0.01$.

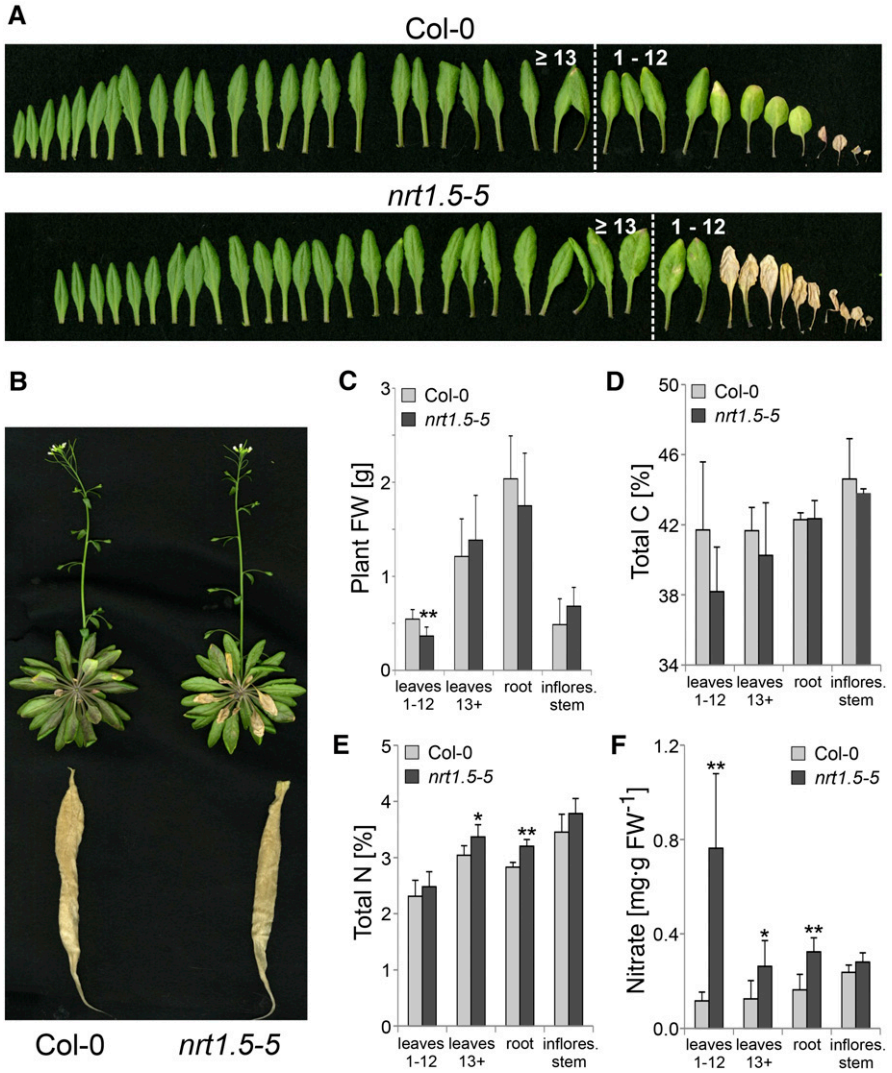

Figure 2. NO_3^- limitation-induced *nrt1.5-5* phenotype in hydroponic culture. A, Individual rosette leaves of Col-0 and *nrt1.5-5* plants grown for 5 weeks in hydroponic culture with 0.1 mM NH_4NO_3 in the medium. Left to right shows young (nos. ≥13) to old (nos. 1–12) leaves. B, Representative picture of Col-0 and *nrt1.5-5* plants at the time of harvest showing the root, the abaxial side of the rosette, and the inflorescence stem. C, Fresh weight (FW) of harvested plant material used for further analyses: pooled old leaves numbers 1 to 12, pooled young leaves numbers ≥13, roots, and inflorescence stems (means ± SD; $n \geq 9$). D, Total C content in said plant material (means ± SD; $n \geq 4$). E, Total N content in said plant material (means ± SD; $n \geq 4$). F, NO_3^- concentration in said plant material (means ± SD; $n \geq 5$). *, Significant differences (Student's *t* test) between *nrt1.5-5* and Col-0 with $P < 0.05$; **, significant differences (Student's *t* test) between *nrt1.5-5* and Col-0 with $P < 0.01$.

whereas Col-0 rosettes with 3% to 4% K were well supplied (Table I). K deficiency is often accompanied by increased tissue concentrations of other cationic elements, which are partially compensating for the charge imbalances in the plant (Leigh and Jones, 1984). Indeed, we observed a remarkable increase in the two macronutrients Ca (1.5- to 3.0-fold) and Mg (1.3- to 2.0-fold) in rosette leaves and inflorescence stems of *nrt1.5-5* plants. The micronutrients Mn, Zn, and Mo were also increased, whereas B was reduced in rosette leaves (Table I).

Other than in shoots, the elemental composition in wild-type and *nrt1.5-5* roots was almost the same (Table I). Apparently, mutant roots were able to absorb all nutrients in sufficient amounts but particularly failed to transfer K^+ to the shoot. In turn, Ca^{2+} and Mg^{2+} were transported with increased efficiency to the aboveground tissues. These data largely resembled the phenotype of the *skor-1* mutant. Gaymard et al. (1998) showed that the disruption of the *SKOR* gene had no effect on the K content in roots but resulted in an approximately 50% decrease in shoot K, which was essentially compensated for by an increase in Ca. Calculating the cationic charge balance further corroborated that Ca^{2+} and Mg^{2+}, similarly as in *skor-1*, compensated for the decline in K^+ in *nrt1.5-5* shoots, whereas the root cation balance remained unchanged (Supplemental Fig. S3). These results showed that limited NO_3^- fertilization of *nrt1.5-5* plants provoked the early senescence phenotype and eventually, resulted in severe K deficiency in the shoot. The comparison with *skor-1* suggested that both NRT1.5 and SKOR might contribute to root-to-shoot translocation of K^+, possibly influenced by the availability and uptake of NO_3^- in the roots.

Transcription of Ion Homeostasis-Associated Genes Indicates K Deficiency in *nrt1.5-5* Shoots

The K deficiency in shoots of *nrt1.5-5* plants grown under low NO_3^- supply in hydroponics could be associated with altered expression of ion transporter or channel genes or selected NO_3^- and K^+ signaling pathway

Table I. *Elemental analysis in tissues of Arabidopsis nrt1.5-5 and Col-0 plants grown in hydroponic culture under supply of 0.1 mM NH_4NO_3 for 5 weeks*

The concentration of macro- and microelements was determined in homogenized material from leaf numbers 1 to 12, leaf numbers ≥13, roots, and inflorescence stems. Bold numbers indicate significantly lower or higher elemental concentration (Student's *t* test; *, $P < 0.05$; and **, $P < 0.01$) in *nrt1.5-5* tissues when compared with Col-0.

Macro- and Microelements	Leaves 1-12		Leaves 13+		Roots		Inflorescence Stem	
	Col-0	*nrt1.5-5*	Col-0	*nrt1.5-5*	Col-0	*nrt1.5-5*	Col-0	*nrt1.5-5*
Macroelements (mg g^{-1} dry wt)								
K	30.7 ± 5.1	**7.9 ± 1.0****	43.8 ± 5.4	**19.5 ± 1.5****	56.5 ± 8.4	55.1 ± 8.0	32.3 ± 5.9	**26.2 ± 3.3***
Ca	17.4 ± 2.7	**30.5 ± 3.6****	7.5 ± 1.6	**21.5 ± 2.2****	0.5 ± 0.4	0.9 ± 0.8	1.7 ± 0.6	**4.6 ± 0.6****
Mg	15.8 ± 1.6	**23.6 ± 2.9****	8.1 ± 0.9	**16.1 ± 1.6****	1.9 ± 0.3	**1.5 ± 0.3***	3.0 ± 0.6	**3.9 ± 0.4****
P	7.8 ± 0.5	**9.1 ± 1.6***	8.0 ± 0.8	8.6 ± 0.8	9.5 ± 1.5	9.7 ± 1.3	8.2 ± 2.2	6.9 ± 0.6
S	6.0 ± 0.6	**8.1 ± 1.5****	8.4 ± 0.5	**10.3 ± 1.0****	10.1 ± 1.7	10.2 ± 1.4	8.0 ± 1.4	8.7 ± 0.9
Microelements (μg g^{-1} dry wt)								
Fe	102.8 ± 44.5	158.4 ± 164.8	81.8 ± 27.7	76.7 ± 20.2	5,375.6 ± 1,842.5	7,125.0 ± 1,586.9	61.4 ± 14.1	56.0 ± 5.1
B	166.8 ± 24.8	**109.6 ± 12.5****	85.9 ± 10.1	**75.9 ± 8.2***	15.6 ± 33.8	28.8 ± 66.7	28.6 ± 10.6	24.1 ± 1.7
Mn	507.9 ± 98.0	**685.1 ± 131.4****	348.1 ± 113.8	**653.1 ± 107.6****	258.0 ± 189.0	178.4 ± 74.9	120.1 ± 30.7	143.5 ± 16.5
Zn	83.7 ± 7.7	**117.2 ± 18.9****	79.1 ± 10.3	**135.5 ± 14.5****	200.7 ± 49.6	235.8 ± 50.9	53.8 ± 14.3	**73.2 ± 7.2****
Mo	24.1 ± 5.7	25.0 ± 5.3	9.9 ± 3.8	**13.8 ± 1.8***	130.8 ± 23.1	**155.6 ± 22.8***	0.4 ± 0.4	0.7 ± 0.1
Cu	6.0 ± 2.0	5.4 ± 1.6	8.7 ± 1.2	7.6 ± 1.3	50.1 ± 12.0	52.3 ± 14.6	4.4 ± 1.2	4.7 ± 1.3

genes in roots. Expression analysis of 48 genes belonging to NO_3^-, K^+, P_i, or NH_4^+ transporter families and a small number of CIPK/CBL family members revealed significant expression changes of five genes that are important contributors in NO_3^-, K^+, or anion transport and one gene encoding a protein kinase involved in the K^+ signaling pathway (Fig. 3), whereas none of the other 42 genes were regulated (Supplemental Table S1). The NO_3^- transporter *NRT1.8* was 32-fold up-regulated in *nrt1.5-5* roots, corroborating earlier findings in *nrt1.5-3 and nrt1.5-4* (Chen et al., 2012). In addition, expression of the membrane protein SLOW ANION CHANNEL-ASSOCIATED1 (SLAC1) HOMOLOG1 (SLAH1), which is likely involved in organic/inorganic anion homeostasis of plant cells (Negi et al., 2008), was strongly increased in *nrt1.5-5* roots (Fig. 3). Also SLAH3, another member of the SLAC1/SLAH channel family, was significantly up-regulated. The protein was previously characterized as a preferentially NO_3^--permeable channel, with activity that is regulated by NO_3^-, calcium, and an abscisic acid-sensitive phosphorylation step (Geiger et al., 2011).

Although the shoot suffered from K deficiency, expression of the high-affinity K^+ transporter *HAK5* was 8-fold lower in mutant roots, and the 3.7-fold up-regulated expression of the voltage-dependent K^+ channel *SKOR* did not compensate for the K deficit in the shoots (Fig. 3; Table I). Moreover, the *CIPK9* gene, a critical K deprivation-inducible regulator of the low K response in Arabidopsis (Pandey et al., 2007; Liu et al., 2013), was 5-fold down-regulated in *nrt1.5-5* roots, suggesting that the *nrt1.5-5* root system was impaired in sensing or responding to K deficiency in the shoot. Considering that the elemental composition in *nrt1.5-5* roots was almost the same as in the wild type (Table I), the root transcript patterns indicate an influence of NRT1.5 on the NO_3^- and K^+ balance between roots and shoot.

Genes involved in biotic stress responses and jasmonic acid (JA) signaling have been described to play a prominent role in K-dependent gene regulation in Arabidopsis (Armengaud et al., 2004). We, therefore, surveyed by quantitative real-time PCR (qPCR) the expression of 20 genes related to JA metabolism in *nrt1.5-5* shoots and another 14 genes related to calcium signaling and other plant stress response pathways, like defense, secondary metabolism, and reactive oxygen species production. Indeed, all 34 tested genes were more than 2-fold up-regulated in *nrt1.5-5* leaves (Supplemental Fig. S4); 26 of the 34 tested genes were reported to be up-regulated in shoots under K starvation (Armengaud et al., 2004), supporting the notion that *nrt1.5-5* mutant shoots sense and respond to K deficiency.

Overall, the transcription data are consistent with the altered K^+ balance in the shoot and root system of *nrt1.5-5* plants, defective shoot-to-root K deficiency signaling, and impaired root-to-shoot translocation of the cation. Our data suggest that *NRT1.5* and the other alternatively regulated root genes are critical actors in these processes. In addition, the up-regulated expression of *SKOR* in *nrt1.5-5* roots supports the idea of an interplay of the two proteins in the root-to-shoot translocation of K^+.

The Presence of NRT1.5 in Roots Is a Prerequisite for Proper Root-to-Shoot Translocation of K^+ under Low NO_3^- Supply

To investigate whether the deficit in K^+ translocation was caused by the root (loading of the xylem) or the shoot (unloading of the xylem), we generated homografted (Col-0 stock/Col-0 scion and *nrt1.5-5* stock/*nrt1.5-5* scion) and heterografted (Col-0 stock/*nrt1.5-5* scion and *nrt1.5-5* stock/Col-0 scion) plants and grew them on low-fertilized soil. The early leaf senescence phenotype of the mutant developed most severely on the *nrt1.5-5* root stock (Fig. 4A), indicating that the absence of NRT1.5 function in the root was primarily responsible for symptom manifestation. This conclusion was corroborated by the observation of reduced shoot K concentrations (<1% of dry weight) on the *nrt1.5-5*

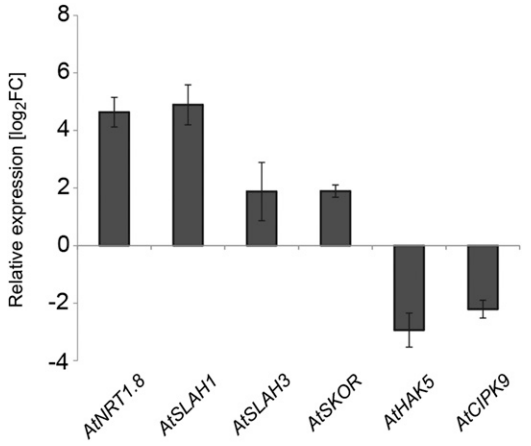

Figure 3. Differentially regulated genes in roots of *nrt1.5-5* plants. Relative transcript levels of six regulated genes in roots of hydroponically grown plants were measured by qPCR and normalized to *UBQ10* (means ± SD; $n = 4$). Plotted are the $\log_2$ fold expression changes (FCs) in *nrt1.5-5* roots compared with Col-0 roots.

root stock, whereas root K concentrations were unchanged, irrespective of the grafting combination (Fig. 4B). Further support came from elevated Ca and Mg concentrations in shoots of grafted plants with an *nrt1.5-5* root stock, suggesting that both cations contributed to compensating for the charge imbalances provoked by K deficiency (Supplemental Fig. S5).

Genetic Complementation of *nrt1.5-5* by Expression of *NRT1.5* under Control of the *PHOSPHATE1* Promoter

For complementation of the *nrt1.5-5* mutant, we transformed the plants with the *NRT1.5* coding region fused behind the promoter of the *PHOSPHATE1* (*PHO1*) gene (At3g23430), with expression that is primarily directed to the root vasculature (Supplemental Note S1; Hamburger et al., 2002; Wege and Poirier, 2014). The transformants expressed approximately wild-type levels of *NRT1.5* transcripts in the roots (Fig. 5A), and the endogenous *PHO1* expression was unchanged (Fig. 5B). Determination of K, Ca, and Mg concentrations in three independent *PHO1p*:*NRT1.5* transformed *nrt1.5-5* lines (1–3) in comparison with Col-0 and *nrt1.5-5* plants revealed a recovery of all three elements to wild-type concentrations in the shoot (Fig. 5C), which finally resulted in wild-type rosette phenotype of the complemented lines (Fig. 5D). This experiment showed that wild-type *NRT1.5* expression in roots is needed to meet the K demand of the shoot.

NRT1.5 Enhances Hygromycin B Sensitivity in Yeast and Plants

To functionally test NRT1.5 in a heterologous expression system for K^+ transport activity, the yeast (*Saccharomyces cerevisiae*) mutants BYT12, lacking the main K^+ uptake systems (*trk1 trk2*), and BYT45, lacking the main K^+ efflux systems (*nha1 ena1*) were used (Zahrádka and Sychrová, 2012). The inward-rectifying Arabidopsis K^+ channel KAT1 and the outward-rectifying K^+ channel SKOR served as positive controls in the yeast assays. NRT1.5 was not able to complement the growth retardation of BYT12 under K deficiency (Fig. 6A) or counteract the accumulation of toxic levels of K^+ in BYT45 cells (Fig. 6B). To test for an interaction of NRT1.5 and SKOR on K^+ efflux, both proteins were coexpressed in BYT45 cells. Yeast growth of the double transformants was indistinguishable to the single transformants with *SKOR*, indicating no direct influence of NRT1.5 on SKOR activity under these conditions in yeast (Fig. 6B).

In yeast, sensitivity to toxic cationic drugs like Hygromycin B (HygB) is often linked to changes in the membrane potential, which can be provoked by alterations in K^+ homeostasis (Barreto et al., 2011). Accordingly, the deletion of both *TRK* genes in BYT12 cells results in a higher sensitivity to toxic cations, even under nonlimiting K^+ concentrations in the medium (Navarrete et al., 2010), because of a hyperpolarization of the plasma membrane. To investigate whether

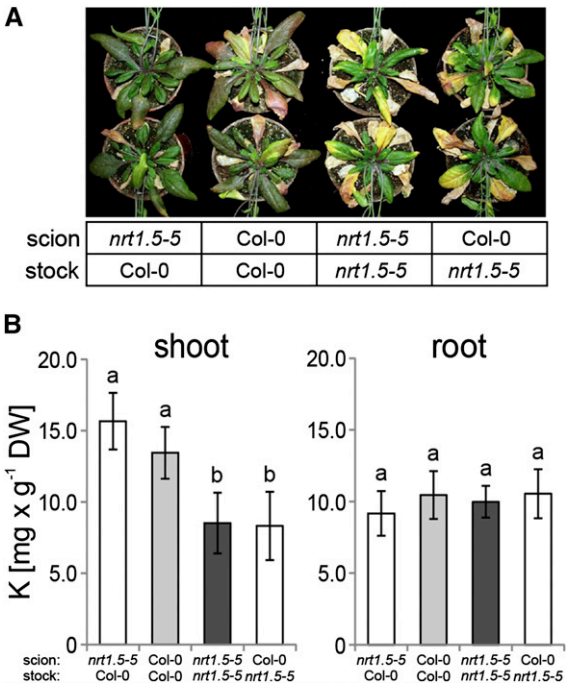

Figure 4. Rosette phenotype and K concentrations in shoots and roots of grafted Arabidopsis plants. A, Early leaf senescence phenotype as a result of the grafts as indicated in lower. Grafted plants were grown for 6 weeks on unfertilized type 0 soil supplemented for the first 2 weeks with 10 mM KNO_3 to support plant growth and subsequently, 1 mM KNO_3 to trigger development of the phenotype. B, K concentrations in shoots and roots of grafted plants. Data are means ± SD ($n \geq 6$). The data were statistically analyzed by one-way ANOVA and subsequent multiple comparisons (Tukey's range test). Different letters indicate a significant difference at $P < 0.05$. Vertical bars denote SDs. DW, Dry weight.

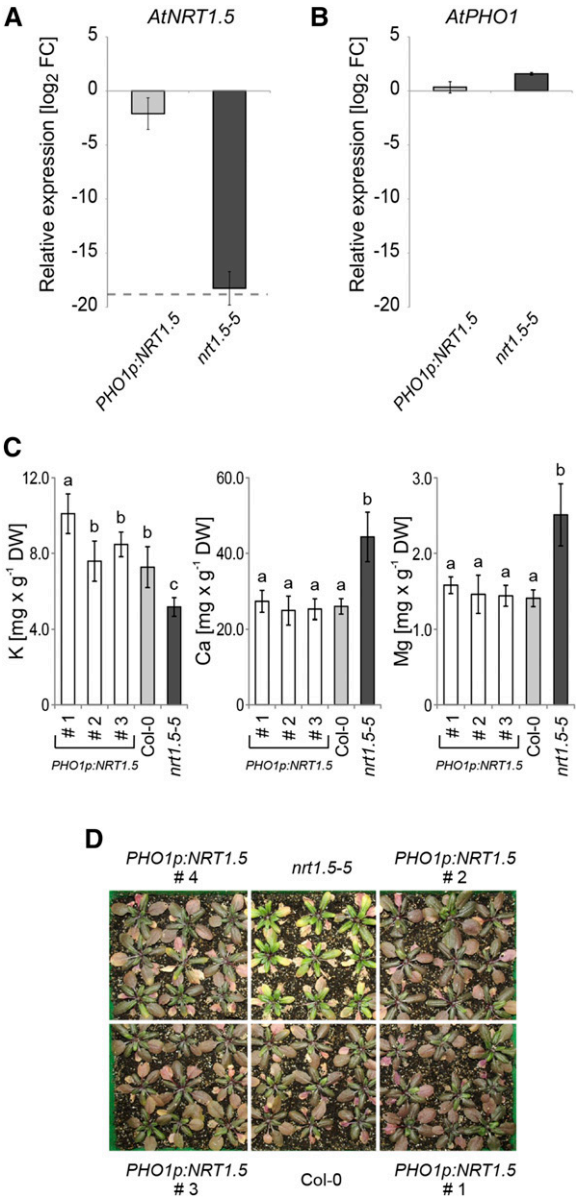

Figure 5. Complementation of the *nrt1.5-5* mutant. A, Relative *NRT1.5* transcript levels in seedling roots of *PHO1p:NRT1.5*-transformed and -nontransformed *nrt1.5-5* plants compared with *NRT1.5* transcript levels in Col-0 plants. *PHO1* promoter-driven expression of *NRT1.5* recovers almost wild-type transcript level in the *nrt1.5-5* mutant background. The *NRT1.5* signal in nontransformed *nrt1.5-5* plants is at background noise level (gray dashed line). B, Relative *PHO1* transcript levels in seedling roots of *PHO1p:NRT1.5*-transformed and -nontransformed *nrt1.5-5* plants compared with *PHO1* transcript levels in Col-0 plants. *PHO1* promoter-driven expression of *NRT1.5* does not alter the *PHO1* transcript level in the *nrt1.5-5* mutant background. Seedlings in A and B were raised in one-half-strength MS liquid culture. Relative transcript levels in A and B were measured by qPCR and normalized to *UBQ10*. Plotted are the $\log_2$ fold expression changes (FCs) compared with Col-0 seedling roots. Values are means ± SD of $n = 6$ independent transgenic *PHO1p:NRT1.5* lines (including lines 1–4 shown in C and D) with eight pooled plants per sample and $n = 3$ *nrt1.5-5* samples with eight pooled plants per sample. C, Potassium, Ca, and Mg concentrations (means ± SD; $n = 9$) in rosettes of Col-0, *nrt1.5*-5, and three independent *PHO1p:NRT1.5*-transformed *nrt1.5-5* lines (1–3) grown on unfertilized type 0 soil and supplemented with a one-half-strength MS-based fertilization solution containing 1:1:10 mM N:K:P (Supplemental Table S2). The data were statistically analyzed by one-way ANOVA and subsequent multiple comparisons (Tukey's honestly significant difference mean-separation test). In samples marked with different letters, concentrations differ significantly at $P < 0.05$. D, Rosette phenotype of *nrt1.5-5*, Col-0, and four independent *PHO1p:NRT1.5*-transformed *nrt1.5-5* lines grown under the same condition as in C. DW, Dry weight.

NRT1.5 has an influence on the plasma membrane potential, we expressed *NRT1.5* in wild-type BY4741 cells and BYT12 cells and observed yeast growth on plates containing an HygB concentration gradient (Fig. 6C). Empty vector controls (p426) confirmed that BYT12 cells were more sensitive to the antibiotic, because they did not grow properly on HygB concentrations above 250 mg L^{-1}. Transformation of BYT12 but not BY4741 cells with NRT1.5 resulted in strongly increased HygB sensitivity. These results suggest that expression of *NRT1.5* causes hyperpolarization of the yeast plasma membrane in the K^+ uptake-deficient mutant, but they do not provide support for K^+ transport activity of NRT1.5.

Remarkably, root growth of *nrt1.5* mutants on one-half-strength Murashige and Skoog medium (MS) was markedly less impaired by HygB than in wild-type seedlings (Fig. 6D), which is in accordance with the result that overexpression of NRT1.5 caused yeast cells to be more susceptible to HygB. Because the membrane potential is the major proton-motive force that drives HygB uptake, we tested the development of *nrt1.5* mutants, *PHO1*:*NRT1.5* complementation lines, and Col-0 plants on one-half-strength MS with additional 50 mM KCl supply, because elevated K concentrations decrease the membrane potential (Hirsch et al., 1998). Indeed, the *nrt1.5* mutants were more sensitive to 50 mM KCl than wild-type plants (Supplemental Fig. S6). Similar responses to HygB and high K concentrations in the medium were previously observed in *plasma membrane proton atpase2* (*aha2*) mutants (Haruta et al., 2010). Moreover, the two independent complementation lines of *nrt1.5-5* developed like the wild type on HygB or 50 mM KCl (Supplemental Fig. S6). Therefore, we speculate that, in *nrt1.5* mutants, the membrane potential is similarly reduced as in *aha2* mutants.

Both NRT1.5 and SKOR Contribute to Shoot K Homeostasis in an NO_3^- Supply-Dependent Manner

To investigate the interplay between NRT1.5 and SKOR on root-to-shoot translocation of K^+ in planta, we isolated the two T-DNA insertion mutants *skor-2* and *skor-3* in the Col-0 background (Supplemental Fig. S7A). Both mutants exhibit the same phenotype (Supplemental Fig. S7C). We crossed *skor-2*, which carries the T-DNA insertion in the essential cyclic

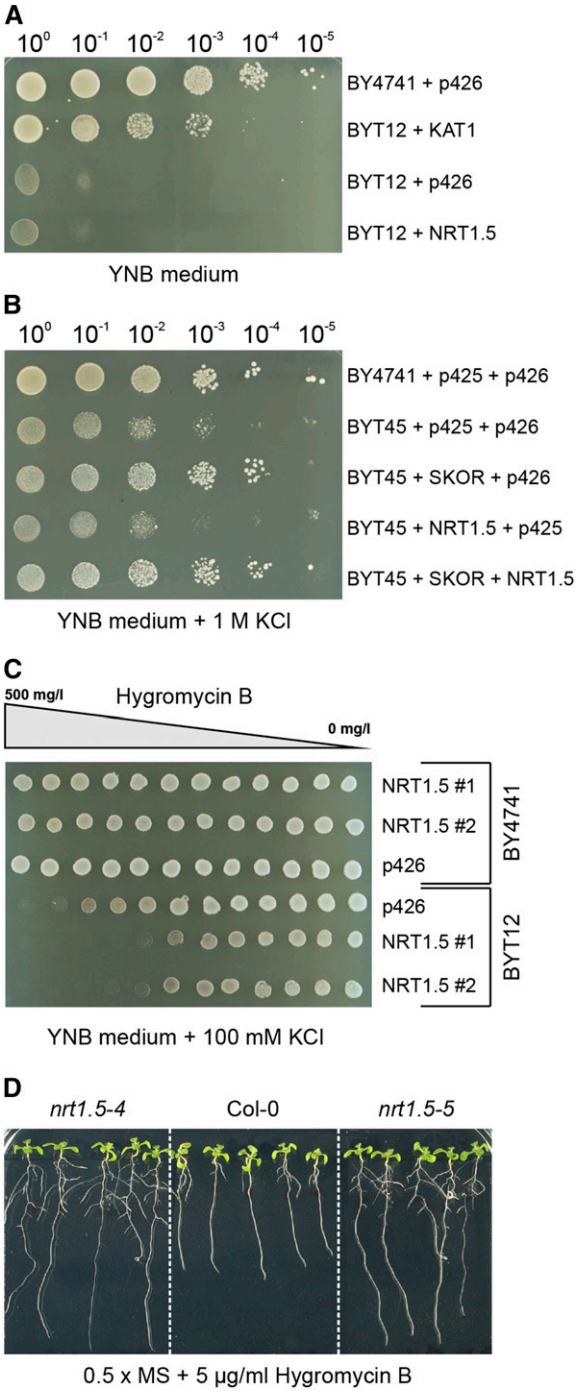

Figure 6. Functional analysis of NRT1.5. A, Potassium uptake capacity was analyzed in yeast BY4741 and the potassium import mutant strain BYT12 (*trk1*Δ *trk2*Δ) and transformed with the expression constructs indicated on the right; 20-μL cell suspensions (OD_{600} from 1.0 to 10^{-5}) were dropped on YNB (-Ura) agar plates containing 7 mM K^+, which is growth limiting for BYT12 cells. p426 is the empty vector. KAT1 and NRT1.5 are coding sequences of the respective Arabidopsis genes cloned in p426. B, Potassium export capacity was analyzed in yeast BY4741 and the potassium export mutant strain BYT45 (*ena1-5*Δ *nha1*Δ) cells and transformed with the expression constructs indicated on the right; 20-μL cell suspensions (OD_{600} from 1.0 to 10^{-5}) were dropped on YNB (-Ura -Leu) agar plates supplemented with 1 M KCl, which is growth suppressing for BYT45 cells. p425 and p426 are empty vectors; SKOR and NRT1.5 are coding sequences of the respective Arabidopsis genes cloned in p425 and p426, respectively. C, HygB sensitivity of yeast BY4741 and BYT12 cells transformed with the expression constructs indicated on the right on YNB (-Ura) agar plates containing 100 mM KCl to support growth of BYT12 and an HygB concentration gradient from 0 to 0.5 g L^{-1}. Twelve 3-μL drops of each yeast cell suspension (OD_{600} = 1.0) were distributed along the HygB gradient on the plate; 1 and 2 indicate two independent yeast transformants. Representative pictures of three independent experiments are shown. D, Root sensitivity test of *nrt1.5* mutants and Col-0 on HygB-containing medium. Seedlings pregerminated for 4 d on one-half-strength MS were transferred on one-half-strength MS containing 5 mg L^{-1} HygB and continued to grow vertically for 7 more d.

nucleotide binding domain (Dreyer et al., 2004), with *nrt1.5-5* to generate a double mutant. Absence of gene-specific full-length transcripts in single and double mutants was verified by reverse transcription (RT)-PCR (Supplemental Fig. S7B). Wild-type Col-0, *nrt1.5-5*, *skor-2*, and *nrt1.5-5/skor-2* plants were cultivated on unfertilized soil supplemented with modified one-half-strength MS solutions containing the macronutrients N (as NO_3^-):K:P in the concentrations 1:1:1, 1:1:10, 1:10:1, 10:1:1, 5:0:5, and 10:10:10 mM, respectively. When all plants were flowering, the inflorescence stems were removed, rosette phenotypes were documented, and the elemental composition was determined by ICP-OES (Fig. 7).

In all four plant lines, early leaf senescence accompanied by yellow leaf tips and pale green inner rosettes occurred whenever the K concentration dropped below 1% dry weight (Fig. 7, red dotted line). At K concentrations of ≥1%, all plants regained the ability to accumulate anthocyanins and developed a red-brown leaf pigmentation that presumably indicated N deficiency (Fig. 7, treatments 1:1:1, 1:1:10, and 1:10:1 mM N:K:P). The concentrations of Ca and Mg in the rosettes were inversely correlated to that of K in all plant lines.

Interestingly, at 1 mM NO_3^- fertilization, the K concentrations in *nrt1.5-5* and *nrt1.5-5/skor-2* plants were reduced to approximately 50% of wild-type and *skor-2* levels, respectively, and even supplying a 10-fold excess of K^+ over NO_3^- could not revert them back to wild-type level (Fig. 7, treatment 1:10:1 mM N:K:P). Obviously, NRT1.5 made an important contribution to the shoot K status when NO_3^- supply is limited, whereas the *skor-2* mutant behaved like the wild type.

Total N concentration in all lines grown at 1 mM NO_3^- supply was less than 2.5% (Fig. 7), which verified the low NO_3^- supply to the plants. Interestingly, when NO_3^- supply is limited, total N in *nrt1.5-5/skor-2* mutant plants was higher than those of the wild type and single mutants. Fresh weight analysis further reflected the importance of NO_3^- supply to plant growth. Under 1 mM NO_3^- supply, the fresh weight gain of all lines was below 110 mg. In contrast, when 10 mM NO_3^- was supplied, fresh weight gain increased 2- to 3-fold.

Under a 10-fold excess of NO_3^- over K^+, the *nrt1.5-5* mutant contained similar K concentrations as wild-type plants (Fig. 7, treatment 10:1:1 mM N:K:P), which

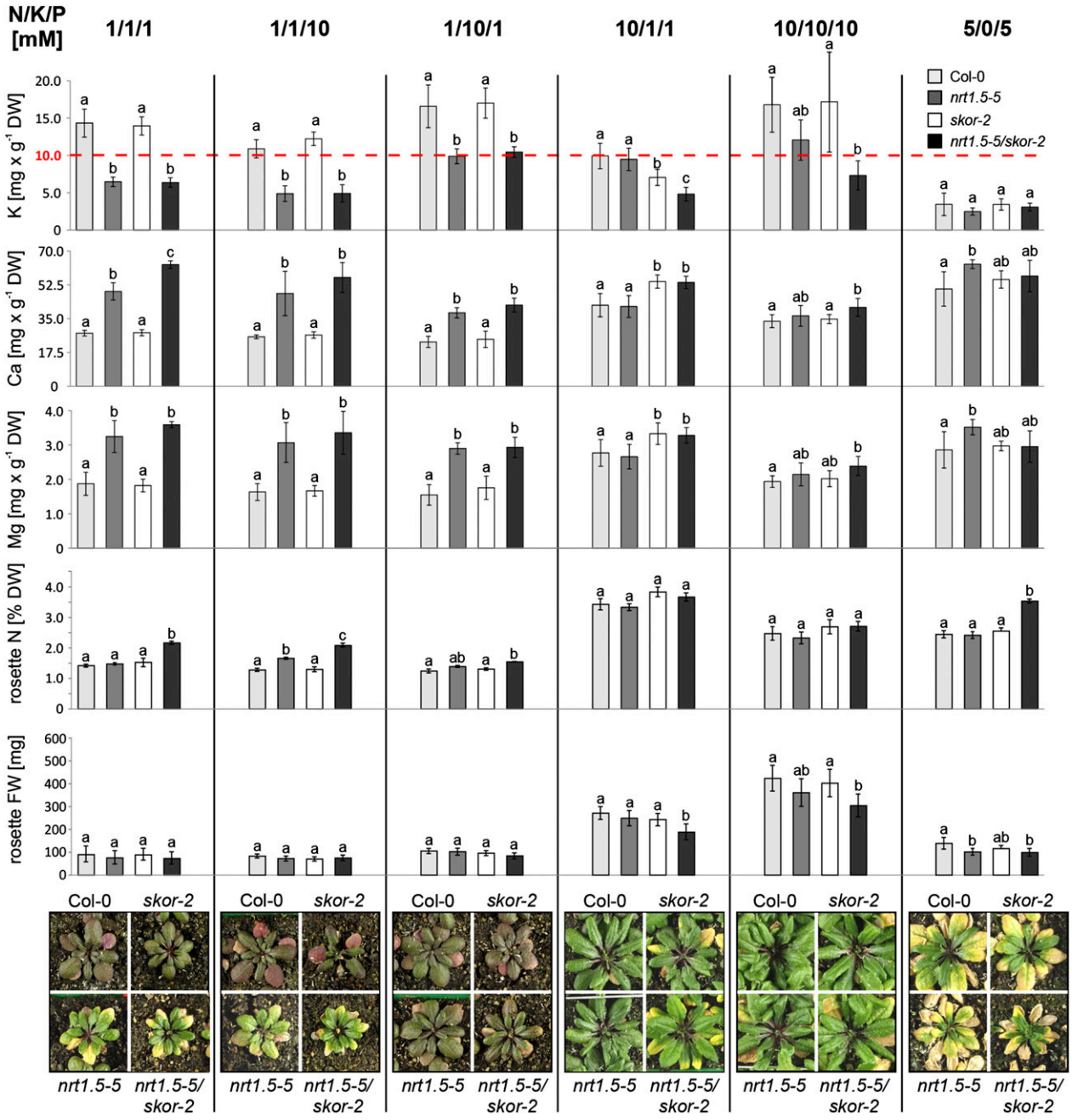

Figure 7. Correlation of the rosette phenotype with the K, Ca, and Mg elemental composition in response to varying N, K, and P supply in Col-0, *nrt1.5-5*, *skor-2*, and *nrt1.5-5/skor-2* plants. Each column shows the applied fertilization regime (N to K to P [mM]) along the top. The bar diagrams show the rosette K, Ca, Mg, and total N concentrations and fresh weight (FW) gain, respectively. On the bottom, the respective phenotypes of the plants are shown. The color codes of the bars are indicated in the top right corner. The dotted red line indicates a K concentration of 1% in the dry matter. The data were statistically analyzed by one-way ANOVA and subsequent multiple comparisons (Tukey's honestly significant difference mean-separation test). Means ($n \geq 4$) marked with different letters differ significantly at $P < 0.05$. Vertical bars denote SDS. The experiment was performed three times independently with similar phenotypic growth responses. The elemental analysis by ICP-OES was performed for two of three independent experiments with similar results. DW, Dry weight.

indicated that NRT1.5 was not primarily involved in the establishment of the shoot K status under these growth conditions. As expected, *skor-2* plants had a significantly lower K concentration compared with Col-0 and *nrt1.5-5*. Lack of both NRT1.5 and SKOR decreased K levels even further. These results were confirmed by treating the *skor-2* and *nrt1.5-5/skor-2* plants with a 20-fold excess of NO_3^- over K^+, which resulted in a similar reduction in shoot K concentration (Supplemental Fig. S8A). Under a high equimolar

supply of NO_3^- and K^+ (i.e. 10:10:10 and 10:10:1 mM N:K:P), both single mutants reached K levels close to Col-0 (Fig. 7; Supplemental Fig. S8B). However, even then the K concentrations in *nrt1.5-5/skor*-2 double mutant were significantly reduced. This highlighted the importance of both proteins for shoot K^+ homeostasis under defined nutritional supply: SKOR under high NO_3^- and low K^+ availability and NRT1.5 under low NO_3^- availability and independent of the K^+ supply. Enhancement of K deficiency in the double mutant under a high NO_3^- to K^+ ratio and a high equimolar supply further suggests an interdependency of NRT1.5 and SKOR in K^+ root-to-shoot translocation under these conditions.

To investigate whether the regulation of *SKOR* and *NRT1.5* in roots under different N to K regimes is consistent with this model, we analyzed their expression in roots of wild-type plants grown on unfertilized soil supplemented with 1:1:1, 10:1:1, 1:10:1, and 10:10:1 mM N:K:P. Expression of *NRT1.5* was only very weakly regulated under the different NO_3^- to K^+ ratios (Supplemental Fig. S9). Relative to equimolar supply (1:1:1 or 10:10:1 mM N:K:P), *NRT1.5* was <1.5-fold up-regulated by high NO_3^- to K^+ ratio (10:1:1 mM N:K:P) and < 1.5-fold down-regulated by low NO_3^- to K^+ ratio (1:10:1 mM N:K:P). In contrast to *NRT1.5*, *SKOR* was, independent of the NO_3^- to K^+ ratio, strongly up-regulated by high NO_3^- supply (10:1:1 and 10:10:1 mM N:K:P). These expression patterns of the two genes could partially explain the phenotypes of the mutant plants, but it is possible that also altered expression of other genes that was observed in *nrt1.5-5* roots (Fig. 3) contributed to the phenotypes. Under low NO_3^- supply (1 mM), expression of *NRT1.5* is nearly constant, whereas expression of *SKOR* is 5-fold lower than under high NO_3^- supply. Consistently, when grown with 1 mM NO_3^-, *nrt1.5-5* but not *skor-2* mutant plants had reduced K levels in the shoots (Fig. 7). In contrast, under high NO_3^- supply (10 mM), *SKOR* is strongly expressed in roots. It is conceivable that, under these conditions, SKOR can partially complement the lack of NRT1.5 in the *nrt1.5* mutants and facilitate root-to-shoot translocation of K^+. This view is concordant with the finding that, under high NO_3^- supply, the K concentrations in *nrt1.5-5* and wild-type plants do not significantly differ (Fig. 7).

DISCUSSION

NRT1.5 Is Required to Maintain Root-to-Shoot Translocation of K^+ under Low NO_3^- Supply

Lin et al. (2008) reported that the NPF member NRT1.5 functions in *X. laevis* oocytes as a low-affinity, pH-dependent bidirectional NO_3^- transporter and participates in plants in root xylem loading with NO_3^-, although in *nrt1.5* mutants root-to-shoot translocation of NO_3^- was not completely blocked. In addition, Lin et al. (2008) observed a reduced K^+ transport to the shoot when NO_3^- and not NH_4^+ was supplied to the mutants and therefore, suggested a homeostatic balance between the anion NO_3^- and the cation K^+ in the xylem stream. Interestingly, we found that K deficiency in the shoot of *nrt1.5-5* mutant plants was most severe under low NO_3^- supply (Figs. 4 and 7), and supplementation of soil with 10 mM NO_3^- (with or without additional supply of K^+; Fig. 7; Supplemental Fig. S8) diminished or even completely abolished the K deficiency of *nrt1.5-5* shoots. This indicated a much more subtle regulation of shoot K^+ homeostasis, involving NRT1.5 and K^+ transporters and channels.

Cation-anion fluxes in the xylem are strictly balanced, and the most important counteranion for K^+ is NO_3^-. However, under conditions of low NO_3^- supply and without causing a concomitant shortage in K^+, NO_3^- can be partially substituted by other anions (inorganic or organic), which then act as counteranions for the transport of K^+ from roots to the shoot (Engels and Marschner, 1992b; Marschner et al., 1997). In this context, it was interesting to observe that the expression of *SLAH1* was strongly up-regulated and that the expression of *SLAH3* was weakly but still significantly up-regulated in *nrt1.5-5* roots (Fig. 3). These slow anion channels belong to the SLAC/SLAH protein family, which consists in Arabidopsis of five members, SLAC1 and SLAH1 to SLAH4 (Barbier-Brygoo et al., 2011). Their up-regulation in *nrt1.5-5* roots might indicate that the proteins can partially substitute the lack of NRT1.5 by facilitating the efflux of anions from the cells of the vasculature toward the xylem stream. This could possibly result in membrane depolarization and thereby, an activation of the xylem-loading K^+ channel SKOR, which was indeed also transcriptionally up-regulated in *nrt1.5-5* (Fig. 3). Although this model could explain the weaker phenotype of the mutant under high NO_3^- supply (Fig. 7; Supplemental Fig. S8), it fails under limited NO_3^- supply, where increased *SLAH1* expression in *nrt1.5-5* roots did not prevent K deficiency in the shoot. Our results suggest that NRT1.5 is important for a continuous root-to-shoot translocation of K^+ under low NO_3^- supply, whereas its absence is less critical for the plant when ample NO_3^- is available.

The *nrt1.5-5* mutant has, even more pronounced under low NO_3^- supply, a slightly higher content of nitrogenous compounds (Figs. 1, H and I and 2, E and F). Interestingly, this coincides with an accumulation of nearly all macro- and microelements in the mutant shoot, whereas the elemental composition in the roots was only marginally altered (Table I). The increased shoot Ca and Mg concentrations could be explained by charge compensation for the reduced amount of K (Leigh and Jones, 1984). The higher N content and the accumulation of other elements, like P and S, might result from impaired remobilization capability of the *nrt1.5-5* shoot, possibly because of the K deficiency. Cycling and recycling of phloem-mobile mineral nutrients, like phosphate, sulfate, and NO_3^-, is also charge balanced by cations mostly in the form of K^+, and the deficiency can therefore directly affect phloem loading and transport (Marschner et al., 1996, 1997).

An increased expression of JA-responsive and stress-related genes was previously described as a response of

Arabidopsis plants suffering from K deficiency (Armengaud et al., 2004). Thus, the altered transcription pattern of selected JA and stress pathway genes in *nrt1.5* shoots likely is a consequence of the reduced amount of K^+ translocated to the shoot. The transcription changes of ion homeostasis-associated genes in roots did not reflect K deficiency. Decreased expression of *CIPK9*, a protein kinase gene with increased expression under K deprivation (Pandey et al., 2007), and *HAK5*, a transporter involved in high-affinity K^+ uptake at external concentration below approximately 100 μM (Rubio et al., 2008) that is up-regulated in wild-type roots during K^+ starvation (Armengaud et al., 2004), rather indicated that the K deficiency status of the shoot was not transmitted to the outer root cell layers, which are responsible for the uptake of the cation from the soil solution (Drew et al., 1990). This assumption is corroborated by earlier results from Engels and Marschner (1992a), who suggested that xylem loading of K^+ is regulated separately from K^+ uptake into the root cells and that the adjustment of root-to-shoot translocation of K^+ to the demand of the shoot is coupled with an altered xylem loading capacity in the root. The increased expression of *SLAH1*, *SLAH3*, *SKOR*, and *NRT1.8* in *nrt1.5-5* roots would fit such a regulatory adjustment of xylem loading capacities (Fig. 3). *SLAH1*, *SKOR*, and *NRT1.8* are primarily expressed in the root vascular cylinder, and SKOR and NRT1.8 were described to have xylem loading or unloading properties, respectively (Gaymard et al., 1998; Negi et al., 2008; Li et al., 2010). The grafting experiment further suggested that the presence of NRT1.5 in the root vasculature is a prerequisite for a proper root-to-shoot translocation of K^+ under NO_3^- limitation and that the shoot itself has no or only a minor influence on the K concentrations in the shoot or the entire root system under those conditions (Fig. 4, A and B). Accordingly, NRT1.5 may be a molecular regulator of the root capacity for xylem loading with K^+ and therefore, responsible for the maintenance of the root-to-shoot translocation of K^+ under limited NO_3^- supply.

NRT1.5: Transporter or Trigger for Root-to-Shoot Translocation of K^+?

A plausible explanation for the physiological consequences observed in *nrt1.5-5* plants would be a K^+ transport function of NRT1.5. However, the complementation studies using yeast *trk1 trk2* mutants did not provide evidence for a direct K^+ import or export function of the protein. Functional characterization of plant K^+ channels with this mutant was sometimes successful (e.g. Anderson et al., 1992; Sentenac et al., 1992; Obata et al., 2007) but failed in other cases, possibly because of an incompatibility of the heterologous expression system (Dreyer et al., 1999) or the dependence of transport activity on a regulatory network involving protein-protein interactions and posttranslational modifications as described (e.g. for SLAC1 and AKT1; Honsbein et al., 2009; Maierhofer et al., 2014). The lack of such modifying activities or appropriate regulators in yeast could explain the negative results obtained with NRT1.5. Alternatively, NRT1.5 might only modulate or influence the activity of other K^+-transporting membrane proteins as a result of its own transport function or subsequent signaling events or through direct protein-protein interaction.

Because NO_3^- also fulfils an important function as a signaling molecule (Krouk et al., 2010), it is conceivable that the transport of only a few NO_3^- molecules through NRT1.5 modifies the K^+ flux through the transporter itself or associated K^+ channel(s). In K^+ uptake-deficient yeast cells with hyperpolarized plasma membranes, NRT1.5 expression resulted in increased membrane hyperpolarization illustrated by the increased HygB sensitivity of the cells (Fig. 6). If *NRT1.5* expression in plant roots is also involved in regulating the plasma membrane potential, plasma membrane polarization changes of pericycle and xylem parenchyma cells in response to fluctuating NO_3^- supply might explain the NRT1.5-triggered alterations in root-to-shoot K^+ transport. This hypothesis is indirectly corroborated by the enhanced HygB tolerance and susceptibility of *nrt1.5-5* mutant plants to high K concentrations. However, it is currently unclear how plasma membrane potential differences in the vascular tissue of *nrt1.5* mutants might be transferred to the outer root cell layers, which are responsible for the uptake of substances (e.g. HygB).

The activity of ion channels can be influenced by membrane polarization. In Arabidopsis, six and two members of the Shaker K^+ channel family are activated by hyperpolarization and depolarization, respectively (for review, see Lebaudy et al., 2007). It is thus tempting to speculate that NRT1.5 modulates translocation of K^+ by indirectly regulating the activity of voltage-dependent potassium channel proteins.

Job Sharing between NRT1.5 and SKOR in NO_3^--Dependent K^+ Translocation

SKOR is presently known as the main xylem loader for root-to-shoot translocation of K^+ (summarized, for example, in Sharma et al., 2013), a conclusion based on the finding that its disruption strongly reduced the K^+ content in the shoot, whereas the K^+ content in the roots remained unaffected (Gaymard et al., 1998). The *nrt1.5-5* mutant displayed a similar phenotype under NO_3^--limiting conditions, although the expression of SKOR was increased in the roots. Thus, an NO_3^--dependent job sharing between SKOR and NRT1.5 in the root-to-shoot translocation of K^+ is conceivable.

The interplay between NRT1.5 and SKOR was further elucidated in a fertilization experiment utilizing single and double T-DNA insertion lines (Fig. 7; Supplemental Fig. S8). Independent of the chlorosis phenotype, under low NO_3^- (1 mM) conditions, the K concentration in *nrt1.5-5* mutants was always lower

than in the wild type and *skor-2*. Even at a 10-fold excess of K^+ over NO_3^-, K levels in *nrt1.5-5* rosettes remained lower than in Col-0 and *skor-2*, indicating that, irrespective of the K^+ supply, primarily NRT1.5 but not SKOR is involved in root-to-shoot translocation of K^+ in a low-NO_3^- environment. Interestingly, the *skor-1* mutant phenotype in the Wassilewskija background differs from *skor-2* in Col-0 (Supplemental Fig. S10). Therefore, the results by Gaymard et al. (1998)—reduced K^+ content in the shoot of *skor-1* plants (grown on substrate with unknown NO_3^- to K^+ ratio)—preclude a direct comparison of the two *skor* mutants.

SKOR activity is influenced by a variety of triggers, including membrane depolarization (Gaymard et al., 1998), pH (Lacombe et al., 2000), intracellular and external K^+ status (Johansson et al., 2006; Liu et al., 2006), and reactive oxygen species in the form of hydrogen peroxide (Garcia-Mata et al., 2010). Here, we show that lack of SKOR results in reduced shoot K concentrations when the mutant grows on soil with a high NO_3^-:K^+ ratio (10:1 or 20:1). It thus seems that SKOR is most important for the cation-anion balance in the xylem and consequently, the root-to-shoot translocation of K^+ when the transport of NO_3^- toward the xylem is not restricted, whereas the supply with the counterion K^+ is limited.

Finally, the importance of both proteins for root-to-shoot translocation of K^+ is illustrated by the observation that, under high equimolar NO_3^- and K^+ supplies (10:10:10 and 10:10:1 mM N:K:P), both single mutants reached K shoot concentrations close to wild-type plants, whereas the *nrt1.5-5/skor-2* double mutant failed to do so. Accordingly, NRT1.5 and SKOR cooperate on K^+ root-to-shoot translocation under certain nutritional conditions, and this cooperation is important for K homeostasis in the shoot. However, root-to-shoot translocation of K^+ was not completely blocked in the double mutant, indicating the activity of additional K^+ transport systems in the vasculature.

CONCLUSION

The transporter NRT1.5 and the channel protein SKOR are both involved in root-to-shoot translocation of K^+ and regulators of shoot K homeostasis. SKOR activity is responsible for K^+ translocation when plants are supplied with ample NO_3^- but low K^+, whereas the presence of NRT1.5 in the root vasculature is needed for K^+ transport to the shoot when little NO_3^- is available to the plant, irrespective of the K^+ supply. The two proteins act synergistically, which is indicated by reduced shoot K levels in the double mutant but not the single mutants. Although the molecular mechanism determining the interplay between SKOR and NRT1.5 activities remains to be uncovered, this study defines the physiological conditions under which these transporters cooperate. Because in yeast and plants, NRT1.5 seems to induce plasma membrane hyperpolarization, it is conceivable that the NO_3^- concentration in pericycle and xylem parenchyma cells regulates NRT1.5 activity in K^+ translocation through membrane polarization changes. The ability of a plant to adapt to varying NO_3^- and K^+ concentrations in the soil is important for its survival. Our results suggest that NRT1.5 and SKOR synergistically contribute to this ability.

MATERIALS AND METHODS

Plant Material and Growth Conditions

Arabidopsis (*Arabidopsis thaliana*) T-DNA insertion lines were obtained from the Arabidopsis Biological Resource Center. The *nrt1.5-2* (SALK_005099), *nrt1.5-4* (SALK_063393), *nrt1.5-5* (GABI_347B03), *skor-2* (GABI_391G12), and *skor-3* (SALK_097435) lines are in the Col-0 background, and the *skor-1* T-DNA insertion line (N3816) is in the Wassilewskija background. Homozygous mutant plants were identified by PCR (primers are listed in Supplemental Table S3). The T-DNA insertion site in *skor-2* was located in exon 8 at codon number 462 by sequencing the PCR product generated with the GABI T-DNA left border primer and the *skor-2* reverse primer (Supplemental Table S3). Plants were grown on either a low-fertilized 1:1 (v/v) mixture of the commercial soil types P and 0 (Einheitserde) or on the unfertilized type 0 soil supplemented with nutrient solutions as indicated. Soil composition is given in Supplemental Table S4. Plants were cultivated in a growth chamber under long-day conditions (16-h/8-h light-dark cycle and 21°C/18°C day-night cycle) with a light intensity of 120 μmol m^{-2} s^{-1} and a relative humidity of 55% to 70%. For the fertilization experiment in Supplemental Figure S2, plants were supplied from 35 to 55 DAS with 10 mM KNO_3 every 3 to 5 d depending on soil humidity. Plant material was harvested 2 to 3 d after fertilization treatments. For the fertilization experiments in Figure 7 and Supplemental Figures S8 and S10, plants were germinated on fertilized soil (type P) after 10- to 14-d seedlings were singled out on unfertilized soil (type 0) in trays and supplied with the respective fertilization solutions (Supplemental Table S2). Plants were irrigated every 5 to 7 d depending on soil humidity. At harvest, inflorescence stems were removed, and the rosette material was frozen in liquid nitrogen. For the root assay, seeds of Col-0, *nrt1.5-4*, and *nrt1.5-5* were surface sterilized, distributed on one-half-strength MS plates containing 1% (w/v) Suc and 0.3% (w/v) Gelrite (pH 5.8), and stratified in darkness for 2 d at 4°C. After 4 d of growth in long-day conditions (16-h/8-h light-dark cycle, 21°C/18°C day-night cycle, and 120 μmol m^{-2} s^{-1}), seedlings were transferred on one-half-strength MS (1% [w/v] Suc and 0.6% [w/v] Gelrite, pH 5.8) containing HygB or KCl and grown vertically for 7 more d.

Plant Growth in Hydroponic Culture

Plants were grown hydroponically under nonsterile conditions in a growth cabinet. Arabidopsis seeds were germinated under short-day conditions and precultured on rockwool moistened with tap water for 1 week. Tap water was substituted in the second and third weeks by one-half-strength nutrient solution containing 0.5 mM KH_2PO_4, 0.5 mM $MgSO_4$, 125 μM K_2SO_4, 125 μM $CaCl_2$, 50 μM Na-Fe-EDTA, 50 μM KCl, 30 μM H_3BO_3, 5 μM $MnSO_4$, 1 μM $ZnSO_4$, 1 μM $CuSO_4$, and 0.7 μM $NaMoO_4$ (pH 5.8) with KOH. Nitrogen was supplied as 0.5 mM KNO_3. In the fourth week, plants were supplied with full-strength hydroponic growth medium (1 mM KH_2PO_4, 1 mM $MgSO_4$, 250 μM K_2SO_4, 250 μM $CaCl_2$, 100 μM Na-Fe-EDTA, 50 μM KCl, 30 μM H_3BO_3, 5 μM $MnSO_4$, 1 μM $ZnSO_4$, 1 μM $CuSO_4$, and 0.7 μM $NaMoO_4$ [pH 5.8] with KOH) containing 1 mM KNO_3. After 4 weeks, plants were transferred into long-day conditions until harvest (week 9), and the plants were further cultivated in the full-strength growth medium, but nitrogen was supplied as 0.1 mM NH_4NO_3. The nutrient solution was renewed once a week during the first 3 weeks, twice in the fourth week, and every second to third day for the following weeks until harvest. Conditions in the growth chambers were as follows: 10-h/14-h light-dark cycle for short-day conditions and 16-h/8-h light-dark cycle for long-day conditions, light intensity 240 μmol m^{-2} s^{-1}, 22°C/18°C day-night temperature cycle, and 70% relative humidity.

RNA Isolation

Total RNA was extracted from frozen plant material using the hot-phenol extraction method (Verwoerd et al., 1989).

Semiquantitative RT-PCR

Semiquantitative RT-PCR was performed on complementary DNA corresponding to 50 to 200 ng of reverse-transcribed total RNA as described previously (Rausch et al., 2004). Gene-specific primer pairs are listed in Supplemental Table S3. PCR products were visualized by agarose gel electrophoresis.

qPCR

Total RNA was DNase I treated according to the manufacturer's instructions (Fermentas). Absence of genomic DNA was subsequently tested by qPCR using gene At5g65080 intron-specific primers. First-strand complementary DNA was synthesized from 2 μg of total RNA using either SuperScript III Reverse Transcriptase (Life Technologies) or RevertAid H Minus Reverse Transcriptase (Life Technologies) and quality controlled. Unless otherwise noted, expression analyses were performed with tissue from separately grown plants in at least three independent replicates. qPCR reactions were conducted on an ABI 7500 Fast Real-Time PCR System (Applied Biosystems) using the Power SYBR Green PCR Master Mix (Applied Biosystems) following the thermal profile: 1 time (95°C for 10 min) and 40 times (95°C for 15 s and 60°C for 1 min). SDS 2.2.1 software (Applied Biosystems) was used for data analysis. Expression values for each gene were normalized to the reference gene At4g05320 (*UBIQUITIN10* [*UBQ10*]), and relative expression levels were determined according to the work by Czechowski et al. (2005). Primer sequences are listed in Supplemental Table S5.

Complementation of *nrt1.5-5* with *PHO1:NRT1.5*

A 1.6-kb genomic fragment upstream of the *PHO1* initiation codon was PCR amplified on genomic Arabidopsis DNA using primers listed in Supplemental Table S3. The amplification product was cloned upstream of the *NRT1.5* coding region in the binary vector pTkan3. The construct was transformed in *nrt1.5-5* plants by the floral dip method (Clough and Bent, 1998). For gene expression analysis of *PHO1p:NRT1.5* plants, seeds of six independent transgenic lines (wild-type and *nrt1.5-5* plants) were germinated on one-half-strength MS plates. After 1 week, eight seedlings per line were transferred into Erlenmeyer flasks containing 10 mL of one-half-strength MS. Plants were cultivated shaking in a growth chamber under long-day conditions (16-h/8-h light-dark cycle and 21°C/18°C day-night cycle) with a light intensity of 120 μmol m^{-2} s^{-1}. One-half-strength MS was exchanged weekly. At 20 DAS, root material was harvested for RNA extraction with TRIsure Reagent (Bioline). Primers for qPCR are listed in Supplemental Table S5. Growth analysis of three transgenic lines in comparison with Col-0 and *nrt1.5-5* was performed on unfertilized soil (Supplemental Table S4) supplemented with the nutrient solution 1:1:10 mM N:K:P (Supplemental Table S2).

Pulse-Amplitude Modulated Fluorometry

Chlorophyll fluorescence was measured with a FluorCam 800MF (Photon Systems Instruments). After a 20-min dark adaptation of the plants, the minimum fluorescence in dark-adapted state was captured. The maximum yield of chlorophyll fluorescence in the dark-adapted state was induced by an 800-ms pulse of saturating white light (2,100 μmol m^{-2} s^{-1}). The maximum quantum yield of PSII photochemistry (F_v/F_m) was calculated.

Chlorophyll Measurements

Thirty milligrams of frozen and homogenized plant material (whole rosettes including dry leaves) was extracted in 1 mL of 80% (v/v) buffered aqueous acetone containing 2.5 mM sodium phosphate buffer (pH 7.8) for 30 min in the dark at 4°C under gentle shaking. After centrifugation for 10 min at 15,000*g* and 4°C, the supernatant was collected and stored at 4°C until the second extraction of the pellet with 500 μL of buffered aqueous acetone was performed. Both supernatants were combined, and the chlorophyll content was measured spectrophotometrically and calculated according to Porra et al., 1989.

Anthocyanin Measurements

Anthocyanin levels were determined basically according to Neff and Chory, 1998; 50 mg of frozen and homogenized plant material was incubated overnight at 4°C under gentle shaking in 300 μL of methanol acidified with 1% (w/v) HCl. After the addition of 200 μL of deionized water, anthocyanins were separated from chlorophylls by addition of 500 μL of chloroform. After centrifugation for 2 min at 15,000*g*, 400 μL of aqueous phase was diluted with 400 μL of acidified methanol, and the anthocyanin concentration was determined by measuring the A_{530} and A_{657} with a spectrophotometer. Anthocyanin concentrations were calculated by subtracting A_{657} from A_{530}.

Nitrate Measurements

Nitrate was determined colorimetrically according to the protocol by Cataldo et al. (1975). Briefly, 30 to 50 mg of frozen and homogenized plant material (whole rosettes including dry leaves or separated young and old leaves) was mixed with 1.0 mL of deionized water and centrifuged for 5 min at 4°C and 12,000*g*; 40 μL of supernatant was mixed with 160 μL of 1% (w/v) salicylic acid in concentrated sulfuric acid. For background measurement, 40 μL of supernatant were mixed with 160 μL of deionized water. After a 20-min incubation on ice, 1.8 mL of cooled 4 M NaOH was added and mixed carefully. When the samples reached room temperature, the A_{410} was determined with a microplate reader (BioTek), and the values were compared to a nitrate standard curve (0–8.0 mM KNO_3).

Determination of the Total N and C Contents

C and N analysis was performed on a EuroEA3000-Single Elemental Analyzer (www.eurovector.it) according to the manufacturer's instructions; 1.5 to 2.5 mg of homogenized and oven-dried (2 d at 85°C) plant material (whole rosettes including dry leaves or separated young and old leaves) was used for each measurement. Data were analyzed with the Callidus 5.1 software.

Seed Lipid and Protein Analyses

Determination of seed lipid and protein content was basically performed according to Reiser et al., 2004; 40 mg of homogenized dry seeds were mixed in a mortar with 1.5 mL of isopropanol. The suspension was transferred to a reaction tube and incubated for 20 h at 8°C on a laboratory shaker. Samples were then centrifuged for 10 min at 12,000*g*, and the supernatants transferred into preweighted reaction tubes. Isopropanol was finally evaporated, and the total lipid content quantified gravimetrically.

For seed protein quantification, 10 mg of dry seeds were homogenized in a mortar with 0.5 mL of extraction buffer (50 mM HEPES, 5 mM $MgCl_2$, pH 7.5, 1% [v/v] Triton X-100, 15% [v/v] glycerol, 2% [w/v] SDS, 1 mM EDTA, and 1% [w/v] phenylmethylsulfonyl fluoride). After 10 min of centrifugation at 12,000*g*, proteins in the supernatant were precipitated with acetone to remove bicinchoninic acid assay interfering substances: 25 μL of supernatant was diluted with 175 μL of deionized water and incubated with 6 volumes of ice-cold acetone for 30 min at −20°C. After 10 min of centrifugation at 16,000*g* and 4°C, protein pellets were dissolved in 200 μL of deionized water. The protein concentration was determined by BCA-Protein Assay (Pierce).

Yeast Growth Assays

The protein coding sequences of *KAT1*, *NRT1.5*, and *SKOR* were PCR amplified with primers containing restriction sites. *SKOR* was cloned in the yeast (*Saccharomyces cerevisiae*) expression vector p425 (Ura3 marker), and *NRT1.5* and *KAT1* were cloned in p426 (Leu-2 marker; Mumberg et al., 1995) behind the constitutive Translational Elongation Factor EF-1α promoter. Primer combinations are listed in Supplemental Table S3. The constructs were transformed in the yeast strain BY4741 (Brachmann et al., 1998), BYT12 (trk1Δ trk2Δ; Petrezselyova et al., 2010), or BYT45 (ena1-5Δ nha1Δ; Navarrete et al., 2010) by the lithium acetate method (Ito et al., 1983). For each combination of two plasmids, two independent double transformants were generated to confirm identical growth properties. For potassium uptake experiments with BYT12 and export experiments with BYT45, transformed yeast cells were pregrown overnight in liquid yeast nitrogen base (YNB) medium supplemented with or without 100 mM KCl, respectively. The next day, the cells were washed with deionized water and resuspended to an optical density at 600 nm wavelength (OD_{600}) value of 1, and 10-fold serial dilutions from OD_{600} of 1 to 10^{-5} were prepared; 20 μL of each dilution was dropped on YNB agar plates supplemented with or without 1 M KCl for export or import experiments, respectively. The HygB sensitivity test was performed according to Petrezselyova et al., 2010; 3 μL of cell suspension (OD_{600} = 1) was spotted on HygB gradient plates consisting of YNB medium supplemented with 100 mM KCl to support growth of mutant BYT12.

Elemental Analyses

The plant material was dried for 48 h at 75°C, weighed into polytetrafluorethylene digestion tubes, and digested in HNO_3 under pressure using a microwave digester (Ultraclave 4; MLS GmbH). The concentrations of macro- and microelements were determined by ICP-OES using an iCAP 6500 Dual OES Spectrometer (Thermo Fischer Scientific). The certified Standard Reference Material 1515 Apple Leaves (National Institute of Standards and Technology) was used for quality control. Letters highlight significantly lower or higher elemental concentration in *nrt1.5-5* tissues when compared with Col-0. Data are means ± SD ($n \geq 9$). Asterisks indicate statistically significant differences (Student's *t* test) between *nrt1.5-5* and Col-0: *, $P < 0.05$; **, $P < 0.01$, respectively.

Grafting

Grafts between *nrt1.5-5* and Col-0 plants were performed according to the root-shoot grafts protocol by Bainbridge et al. (2006).

Supplemental Data

The following supplemental materials are available.

Supplemental Figure S1. Genomic structure and phenotypes of mutant lines *nrt1.5-2*, *nrt1.5-4*, and *nrt1.5-5*.

Supplemental Figure S2. Supplementation with 10 mM KNO_3 suppressed the pleiotrophic *nrt1.5-5* phenotype on low-fertilized soil.

Supplemental Figure S3. Altered cation distribution in *nrt1.5-5* plants.

Supplemental Figure S4. Expression analysis of JA metabolism-related, Ca-related, and other genes in Col-0 and *nrt1.5-5* leaves.

Supplemental Figure S5. Ca and Mg concentrations in shoots and roots of grafted Arabidopsis plants.

Supplemental Figure S6. Root growth phenotypes of *nrt1.5* mutants in response to HygB and 50 mM KCl.

Supplemental Figure S7. Identification of the T-DNA insertion mutant *skor-2* in the Col-0 background and confirmation of the absence of full-length transcripts in *skor-2* and the double mutant *nrt1.5-5/skor-2*.

Supplemental Figure S8. Rosette phenotype and K, Ca, and Mg concentrations in *nrt1.5-5*, *skor-2*, *nrt1.5-5/skor-2*, and Col-0 plants after 20:1:1 and 10:10:1 mM N:K:P supply, respectively.

Supplemental Figure S9. Expression of *NRT1.5* and *SKOR* under the different NO_3^- to K^+ ratios.

Supplemental Figure S10. Phenotypic differences between *skor* mutants in Arabidopsis accessions Col-0 and Wassilewskija.

Supplemental Table S1. Ion transporter and signaling genes with similar expression levels in roots of *nrt1.5-5* and Col-0 plants grown in hydroponic culture.

Supplemental Table S2. Composition of N, K, and P fertilization solutions.

Supplemental Table S3. Primer sequences for T-DNA insertion lines, RT-PCR, cloning, and complementation analysis.

Supplemental Table S4. Results of soil composition analysis performed by a certified analytical laboratory.

Supplemental Table S5. qPCR primer sequences.

Supplemental Note S1. Choice of the *PHO1* promoter for complementation.

ACKNOWLEDGMENTS

We thank Eva Häffner for help with the statistical analysis (ANOVA), Susanne Reiner for technical assistance with the ICP-OES measurements, Manfred Forstreuter and Sabine Artelt for technical assistance with the C:N analyzer, Hana Sychrova for providing the yeast strains BYT12 and BYT45, and Guillaume Pilot for the binary vectors pUTkan3 and pTkan3.

Received July 22, 2015; accepted October 25, 2015; published October 27, 2015.

LITERATURE CITED

Anderson JA, Huprikar SS, Kochian LV, Lucas WJ, Gaber RF (1992) Functional expression of a probable *Arabidopsis thaliana* potassium channel in *Saccharomyces cerevisiae*. Proc Natl Acad Sci USA **89:** 3736–3740

Armengaud P, Breitling R, Amtmann A (2004) The potassium-dependent transcriptome of Arabidopsis reveals a prominent role of jasmonic acid in nutrient signaling. Plant Physiol **136:** 2556–2576

Bainbridge K, Bennett T, Turnbull C, Leyser O (2006) Grafting. Methods Mol Biol **323:** 39–44

Barbier-Brygoo H, De Angeli A, Filleur S, Frachisse JM, Gambale F, Thomine S, Wege S (2011) Anion channels/transporters in plants: from molecular bases to regulatory networks. Annu Rev Plant Biol **62:** 25–51

Barneix AJ, Breteler H (1985) Effect of cations on uptake, translocation and reduction of nitrate in wheat seedlings. New Phytol **99:** 367–379

Barreto L, Canadell D, Petrezsélyová S, Navarrete C, Maresová L, Peréz-Valle J, Herrera R, Olier I, Giraldo J, Sychrová H, et al (2011) A genomewide screen for tolerance to cationic drugs reveals genes important for potassium homeostasis in *Saccharomyces cerevisiae*. Eukaryot Cell **10:** 1241–1250

Ben Zioni A, Vaadia Y, Herman Lips S (1971) Nitrate uptake by roots as regulated by nitrate reduction products of shoot. Physiol Plant **24:** 288–290

Blevins DG, Barnett NM, Frost WB (1978) Role of potassium and malate in nitrate uptake and translocation by wheat seedlings. Plant Physiol **62:** 784–788

Brachmann CB, Davies A, Cost GJ, Caputo E, Li J, Hieter P, Boeke JD (1998) Designer deletion strains derived from *Saccharomyces cerevisiae* S288C: a useful set of strains and plasmids for PCR-mediated gene disruption and other applications. Yeast **14:** 115–132

Cataldo DA, Haroon M, Schrader LE, Youngs VL (1975) Rapid colorimetric determination of nitrate in plant-tissue by nitration of salicylic-acid. Commun Soil Sci Plant Anal **6:** 71–80

Chen CZ, Lv XF, Li JY, Yi HY, Gong JM (2012) Arabidopsis NRT1.5 is another essential component in the regulation of nitrate reallocation and stress tolerance. Plant Physiol **159:** 1582–1590

Clough SJ, Bent AF (1998) Floral dip: a simplified method for *Agrobacterium*-mediated transformation of *Arabidopsis thaliana*. Plant J **16:** 735–743

Czechowski T, Stitt M, Altmann T, Udvardi MK, Scheible WR (2005) Genome-wide identification and testing of superior reference genes for transcript normalization in Arabidopsis. Plant Physiol **139:** 5–17

Drew MC, Webb J, Saker LR (1990) Regulation of K+ uptake and transport to the xylem in barley roots: K+ distribution determined by electron-probe x-ray-microanalysis of frozen-hydrated cells. J Exp Bot **41:** 815–825

Dreyer I, Horeau C, Lemaillet G, Zimmermann S, Bush DR, Rodriguez-Navarro A, Schachtman DP, Spalding EP, Sentenac H, Gaber RF (1999) Identification and characterization of plant transporters using heterologous expression systems. J Exp Bot **50:** 1073–1087

Dreyer I, Porée F, Schneider A, Mittelstädt J, Bertl A, Sentenac H, Thibaud JB, Mueller-Roeber B (2004) Assembly of plant Shaker-like K(out) channels requires two distinct sites of the channel alpha-subunit. Biophys J **87:** 858–872

Engels C, Marschner H (1992a) Adaptation of potassium translocation into the shoot of maize (*Zea mays*) to shoot demand: evidence for xylem loading as a regulating step. Physiol Plant **86:** 263–268

Engels C, Marschner H (1992b) Root to shoot translocation of macronutrients in relation to shoot demand in maize (*Zea mays L*) grown at different root zone temperatures. Zeitschrift für Pflanzenernährung und Bodenkunde **155:** 121–128

Engels C, Marschner H (1993) Influence of the form of nitrogen supply on root uptake and translocation of cations in the xylem exudate of maize (*Zea Mays L.*). J Exp Bot **44:** 1695–1701

Garcia-Mata C, Wang J, Gajdanowicz P, Gonzalez W, Hills A, Donald N, Riedelsberger J, Amtmann A, Dreyer I, Blatt MR (2010) A minimal cysteine motif required to activate the SKOR K^+ channel of Arabidopsis by the reactive oxygen species H_2O_2. J Biol Chem **285:** 29286–29294

Gaymard F, Pilot G, Lacombe B, Bouchez D, Bruneau D, Boucherez J, Michaux-Ferrière N, Thibaud JB, Sentenac H (1998) Identification and disruption of a plant shaker-like outward channel involved in K^+ release into the xylem sap. Cell **94:** 647–655

Geiger D, Maierhofer T, Al-Rasheid KA, Scherzer S, Mumm P, Liese A, Ache P, Wellmann C, Marten I, Grill E, et al (2011) Stomatal closure by fast abscisic acid signaling is mediated by the guard cell anion channel SLAH3 and the receptor RCAR1. Sci Signal **4:** ra32

Gierth M, Mäser P (2007) Potassium transporters in plants: involvement in K^+ acquisition, redistribution and homeostasis. FEBS Lett **581:** 2348–2356

Gomez-Porras JL, Riaño-Pachón DM, Benito B, Haro R, Sklodowski K, Rodríguez-Navarro A, Dreyer I (2012) Phylogenetic analysis of k(+) transporters in bryophytes, lycophytes, and flowering plants indicates a specialization of vascular plants. Front Plant Sci **3:** 167

Hamburger D, Rezzonico E, MacDonald-Comber Petétot J, Somerville C, Poirier Y (2002) Identification and characterization of the *Arabidopsis PHO1* gene involved in phosphate loading to the xylem. Plant Cell **14:** 889–902

Haruta M, Burch HL, Nelson RB, Barrett-Wilt G, Kline KG, Mohsin SB, Young JC, Otegui MS, Sussman MR (2010) Molecular characterization of mutant Arabidopsis plants with reduced plasma membrane proton pump activity. J Biol Chem **285:** 17918–17929

Hirsch RE, Lewis BD, Spalding EP, Sussman MR (1998) A role for the AKT1 potassium channel in plant nutrition. Science **280:** 918–921

Ho CH, Lin SH, Hu HC, Tsay YF (2009) CHL1 functions as a nitrate sensor in plants. Cell **138:** 1184–1194

Honsbein A, Sokolovski S, Grefen C, Campanoni P, Pratelli R, Paneque M, Chen Z, Johansson I, Blatt MR (2009) A tripartite SNARE-K^+ channel complex mediates in channel-dependent K^+ nutrition in *Arabidopsis*. Plant Cell **21:** 2859–2877

Hörtensteiner S, Feller U (2002) Nitrogen metabolism and remobilization during senescence. J Exp Bot **53:** 927–937

Ito H, Fukuda Y, Murata K, Kimura A (1983) Transformation of intact yeast cells treated with alkali cations. J Bacteriol **153:** 163–168

Johansson I, Wulfetange K, Porée F, Michard E, Gajdanowicz P, Lacombe B, Sentenac H, Thibaud JB, Mueller-Roeber B, Blatt MR, et al (2006) External K^+ modulates the activity of the Arabidopsis potassium channel SKOR via an unusual mechanism. Plant J **46:** 269–281

Krouk G, Crawford NM, Coruzzi GM, Tsay YF (2010) Nitrate signaling: adaptation to fluctuating environments. Curr Opin Plant Biol **13:** 266–273

Lacombe B, Pilot G, Gaymard F, Sentenac H, Thibaud JB (2000) pH control of the plant outwardly-rectifying potassium channel SKOR. FEBS Lett **466:** 351–354

Lebaudy A, Véry AA, Sentenac H (2007) K+ channel activity in plants: genes, regulations and functions. FEBS Lett **581:** 2357–2366

Leigh RA, Jones RGW (1984) A hypothesis relating critical potassium concentrations for growth to the distribution and functions of this ion in the plant cell. New Phytol **97:** 1–13

Léran S, Muños S, Brachet C, Tillard P, Gojon A, Lacombe B (2013) Arabidopsis NRT1.1 is a bidirectional transporter involved in root-to-shoot nitrate translocation. Mol Plant **6:** 1984–1987

Léran S, Varala K, Boyer JC, Chiurazzi M, Crawford N, Daniel-Vedele F, David L, Dickstein R, Fernandez E, Forde B, et al (2014) A unified nomenclature of NITRATE TRANSPORTER 1/PEPTIDE TRANSPORTER family members in plants. Trends Plant Sci **19:** 5–9

Li JY, Fu YL, Pike SM, Bao J, Tian W, Zhang Y, Chen CZ, Zhang Y, Li HM, Huang J, et al (2010) The *Arabidopsis* nitrate transporter NRT1.8 functions in nitrate removal from the xylem sap and mediates cadmium tolerance. Plant Cell **22:** 1633–1646

Lin SH, Kuo HF, Canivenc G, Lin CS, Lepetit M, Hsu PK, Tillard P, Lin HL, Wang YY, Tsai CB, et al (2008) Mutation of the *Arabidopsis* NRT1.5 nitrate transporter causes defective root-to-shoot nitrate transport. Plant Cell **20:** 2514–2528

Liu K, Li L, Luan S (2006) Intracellular K^+ sensing of SKOR, a Shaker-type K^+ channel from Arabidopsis. Plant J **46:** 260–268

Liu LL, Ren HM, Chen LQ, Wang Y, Wu WH (2013) A protein kinase, Calcineurin B-Like Protein-Interacting Protein Kinase9, interacts with calcium sensor Calcineurin B-Like Protein3 and regulates potassium homeostasis under low-potassium stress in Arabidopsis. Plant Physiol **161:** 266–277

Maathuis FJM (2009) Physiological functions of mineral macronutrients. Curr Opin Plant Biol **12:** 250–258

Maierhofer T, Diekmann M, Offenborn JN, Lind C, Bauer H, Hashimoto K, S Al-Rasheid KA, Luan S, Kudla J, Geiger D, et al (2014) Site- and kinase-specific phosphorylation-mediated activation of SLAC1, a guard cell anion channel stimulated by abscisic acid. Sci Signal **7:** ra86

Marschner H, Kirkby EA, Cakmak I (1996) Effect of mineral nutritional status on shoot-root partitioning of photoassimilates and cycling of mineral nutrients. J Exp Bot **47:** 1255–1263

Marschner H, Kirkby EA, Engels C (1997) Importance of cycling and recycling of mineral nutrients within plants for growth and development. Bot Acta **110:** 265–273

Marschner P (2012) Marschner's Mineral Nutrition of Higher Plants. Academic Press, London

Mumberg D, Müller R, Funk M (1995) Yeast vectors for the controlled expression of heterologous proteins in different genetic backgrounds. Gene **156:** 119–122

Navarrete C, Petrezsélyová S, Barreto L, Martínez JL, Zahrádka J, Ariño J, Sychrová H, Ramos J (2010) Lack of main K^+ uptake systems in *Saccharomyces cerevisiae* cells affects yeast performance in both potassium-sufficient and potassium-limiting conditions. FEMS Yeast Res **10:** 508–517

Neff MM, Chory J (1998) Genetic interactions between phytochrome A, phytochrome B, and cryptochrome 1 during Arabidopsis development. Plant Physiol **118:** 27–35

Negi J, Matsuda O, Nagasawa T, Oba Y, Takahashi H, Kawai-Yamada M, Uchimiya H, Hashimoto M, Iba K (2008) CO_2 regulator SLAC1 and its homologues are essential for anion homeostasis in plant cells. Nature **452:** 483–486

Obata T, Kitamoto HK, Nakamura A, Fukuda A, Tanaka Y (2007) Rice shaker potassium channel OsKAT1 confers tolerance to salinity stress on yeast and rice cells. Plant Physiol **144:** 1978–1985

Pandey GK, Cheong YH, Kim BG, Grant JJ, Li L, Luan S (2007) CIPK9: a calcium sensor-interacting protein kinase required for low-potassium tolerance in Arabidopsis. Cell Res **17:** 411–421

Park J, Kim YY, Martinoia E, Lee Y (2008) Long-distance transporters of inorganic nutrients in plants. J Plant Biol **51:** 240–247

Petrezselyova S, Zahradka J, Sychrova H (2010) *Saccharomyces cerevisiae* BY4741 and W303-1A laboratory strains differ in salt tolerance. Fungal Biol **114:** 144–150

Pilot G, Gaymard F, Mouline K, Chérel I, Sentenac H (2003) Regulated expression of Arabidopsis shaker K^+ channel genes involved in K^+ uptake and distribution in the plant. Plant Mol Biol **51:** 773–787

Poirier Y, Thoma S, Somerville C, Schiefelbein J (1991) Mutant of Arabidopsis deficient in xylem loading of phosphate. Plant Physiol **97:** 1087–1093

Porra RJ, Thompson WA, Kriedemann PE (1989) Determination of accurate extinction coefficients and simultaneous equations for assaying chlorophylls a and b extracted with four different solvents: verification of the concentration of chlorophyll standards by atomic absorption spectroscopy. Biochim Biophys Acta-Bioenergetics **975:** 384–394

Rausch C, Zimmermann P, Amrhein N, Bucher M (2004) Expression analysis suggests novel roles for the plastidic phosphate transporter Pht2;1 in auto- and heterotrophic tissues in potato and Arabidopsis. Plant J **39:** 13–28

Reiser J, Linka N, Lemke L, Jeblick W, Neuhaus HE (2004) Molecular physiological analysis of the two plastidic ATP/ADP transporters from Arabidopsis. Plant Physiol **136:** 3524–3536

Rubio F, Nieves-Cordones M, Alemán F, Martínez V (2008) Relative contribution of AtHAK5 and AtAKT1 to K^+ uptake in the high-affinity range of concentrations. Physiol Plant **134:** 598–608

Sentenac H, Bonneaud N, Minet M, Lacroute F, Salmon JM, Gaymard F, Grignon C (1992) Cloning and expression in yeast of a plant potassium ion transport system. Science **256:** 663–665

Sharma T, Dreyer I, Riedelsberger J (2013) The role of K(+) channels in uptake and redistribution of potassium in the model plant *Arabidopsis thaliana*. Front Plant Sci **4:** 224

Takano J, Noguchi K, Yasumori M, Kobayashi M, Gajdos Z, Miwa K, Hayashi H, Yoneyama T, Fujiwara T (2002) Arabidopsis boron transporter for xylem loading. Nature **420:** 337–340

Verwoerd TC, Dekker BMM, Hoekema A (1989) A small-scale procedure for the rapid isolation of plant RNAs. Nucleic Acids Res **17:** 2362

Wang YY, Hsu PK, Tsay YF (2012) Uptake, allocation and signaling of nitrate. Trends Plant Sci **17:** 458–467

Wege S, Poirier Y (2014) Expression of the mammalian Xenotropic Polytropic Virus Receptor 1 (XPR1) in tobacco leaves leads to phosphate export. FEBS Lett **588:** 482–489

Xu J, Li HD, Chen LQ, Wang Y, Liu LL, He L, Wu WH (2006) A protein kinase, interacting with two calcineurin B-like proteins, regulates K^+ transporter AKT1 in Arabidopsis. Cell **125:** 1347–1360

Zahrádka J, Sychrová H (2012) Plasma-membrane hyperpolarization diminishes the cation efflux via Nha1 antiporter and Ena ATPase under potassium-limiting conditions. FEMS Yeast Res **12:** 439–446